

# Cish actively silences TCR signaling in CD8<sup>+</sup> T cells to maintain tumor tolerance

Douglas C. Palmer,<sup>1\*</sup> Geoffrey C. Guittard,<sup>1\*</sup> Zulmarie Franco,<sup>1</sup> Joseph G. Crompton,<sup>1</sup> Robert L. Eil,<sup>1</sup> Shashank J. Patel,<sup>1</sup> Yun Ji,<sup>1</sup> Nicholas Van Panhuys,<sup>2</sup> Christopher A. Klebanoff,<sup>1</sup> Madhusudhanan Sukumar,<sup>1</sup> David Clever,<sup>1,3</sup> Anna Chichura,<sup>1</sup> Rahul Roychoudhuri,<sup>1</sup> Rajat Varma,<sup>2</sup> Ena Wang,<sup>4</sup> Luca Gattinoni,<sup>1</sup> Francesco M. Marincola,<sup>4</sup> Lakshmi Balagopalan,<sup>1</sup> Lawrence E. Samelson,<sup>1</sup> and Nicholas P. Restifo<sup>1</sup>

<sup>1</sup>National Cancer Institute, Bethesda, MD 20892

<sup>2</sup>National Institute of Allergy and Infectious Disease, Bethesda, MD 20892

<sup>3</sup>Medical Scientist Training Program, The Ohio State University College of Medicine, Columbus, OH 43210

<sup>4</sup>Sidra Medical and Research Center, Doha, Qatar

**Improving the functional avidity of effector T cells is critical in overcoming inhibitory factors within the tumor microenvironment and eliciting tumor regression. We have found that Cish, a member of the suppressor of cytokine signaling (SOCS) family, is induced by TCR stimulation in CD8<sup>+</sup> T cells and inhibits their functional avidity against tumors. Genetic deletion of Cish in CD8<sup>+</sup> T cells enhances their expansion, functional avidity, and cytokine polyfunctionality, resulting in pronounced and durable regression of established tumors. Although Cish is commonly thought to block STAT5 activation, we found that the primary molecular basis of Cish suppression is through inhibition of TCR signaling. Cish physically interacts with the TCR intermediate PLC- $\gamma$ 1, targeting it for proteasomal degradation after TCR stimulation. These findings establish a novel targetable interaction that regulates the functional avidity of tumor-specific CD8<sup>+</sup> T cells and can be manipulated to improve adoptive cancer immunotherapy.**

Immunotherapy is potentially curative for patients with advanced hematological and solid malignancies (Restifo et al., 2012; Kalos and June, 2013). CD8<sup>+</sup> T cells play a prominent role in tumor clearance (Arens and Schoenberger, 2010; Zhang and Bevan, 2011), targeting tumor cells for destruction through use of effector molecules such as IFN- $\gamma$ , TNF, and granzymes after ligation of their TCRs. However, this process is often blunted, and tumor-specific CD8<sup>+</sup> T cells fail to mediate tumor regression despite their pronounced infiltration and the presence of cognate antigens (Ohashi et al., 1991; Kaech et al., 2002b; Mortarini et al., 2003; Overwijk et al., 2003; Zippelius et al., 2004; Rosenberg et al., 2005; Harlin et al., 2006; Dranoff and Fearon, 2013). The reasons underlying this state of peripheral tolerance have largely been attributed to the negative regulatory milieu of the tumor microenvironment, inhibitory ligands, and diminished TCR signaling (Whiteside, 2006; Rabinovich et al., 2007; Janicki et al., 2008; Vazquez-Cintron et al., 2010; Gajewski et al., 2013; Maus et al., 2014). Many efforts to enhance antigen reactivity and circumvent this peripheral tolerance have focused on increasing

TCR signal strength and generating highly functionally avid T cells. Strategies to bypass tolerance and increase avidity include TCR derivation from humanized HLA transgenic mice, affinity maturation using phage display, or amino acid substitution using alanine screening (Zhao et al., 2007; Malecek et al., 2013). However these approaches are time consuming and many of the generated receptors elicit host rejection (Davis et al., 2010) and off-target toxicities (Linette et al., 2013; Morgan et al., 2013). Furthermore, this is not tenable in the case of tumor-infiltrating lymphocytes (TILs) that contain polyclonal populations of T cells with low-affinity TCRs. Thus, it remains of paramount importance to identify novel targetable pathways to improve functional avidity to tumor antigens and, ultimately, sustained tumor killing.

The suppressors of cytokine signaling (SOCS) family, which consists of eight members (Socs1–7 and Cish), has long been observed to be involved in immune regulation (Endo et al., 1997; Naka et al., 1997; Starr et al., 1997; Hilton et al., 1998). Socs1 and Socs3 in particular were found to have nonredundant roles in immunity, with immune-specific knockouts having aberrant T cell activation and skewed differentiation (Seki et al., 2003; Catlett and Hedrick, 2005; Davey et al., 2005; Tanaka et al., 2008; Taleb et al., 2009; Dudda et al., 2013). More recently, we have found that the

\*D.C. Palmer and G.C. Guittard contributed equally to this paper.

Correspondence to Douglas C. Palmer: palmerd@mail.nih.gov; or Nicholas P. Restifo: restifo@nih.gov

Abbreviations used: ACT, adoptive cell transfer; Cish, cytokine-induced SH2 protein; ICS, intracellular cytokine staining; PLC- $\gamma$ 1, phospholipase C $\gamma$ 1; rVV, recombinant vaccinia virus; shmiR, short hairpin microRNA; SOCS, suppressor of cytokine signaling; STAT5, signal transducer and activator of transcription 5; TIL, tumor-infiltrating lymphocyte.

This article is distributed under the terms of an Attribution-Noncommercial-Share Alike-No Mirror Sites license for the first six months after the publication date (see <http://www.rupress.org/terms>). After six months it is available under a Creative Commons License (Attribution-Noncommercial-Share Alike 3.0 Unported license, as described at <http://creativecommons.org/licenses/by-nc-sa/3.0/>).

knockdown of Socs1 in adoptively transferred CD8<sup>+</sup> T cells can improve their tumor-killing ability (Palmer and Restifo, 2009; Dudda et al., 2013), whereas the role of other SOCS members in cancer immunology remain largely unknown (Palmer and Restifo, 2009).

We thought that targeting Cish, the founding member of the SOCS family, may have therapeutic potential for cancer immunotherapy. Cish is induced in T lymphocytes after TCR stimulation (Matsumoto et al., 1997; Li et al., 2000) or after the addition of cytokines such as IL-2 (Yoshimura et al., 1995; Jin et al., 2006). However, unlike Socs1, its role in immune regulation is less clear. Cish has been implicated as a positive regulator of CD4<sup>+</sup> T cell proliferation (Li et al., 2000) and, conversely, as a negative regulator of CD4<sup>+</sup> T cell-mediated allergic response (Yang et al., 2013). In the latter study, mice developed a late Th9-associated allergic immune response. More recently, polymorphisms in the *CISH* locus were found to be associated with susceptibility of several human infectious diseases (Khor et al., 2010; Tong et al., 2012); however, the immunological basis for this remains unclear. Even less clear is the molecular means in which Cish regulates immune function. The SOCS family of molecules all share a central SH2 domain and a C-terminal SOCS box, and are thought to negatively regulate cytokine signaling by sequestering activating signaling cascade components such as Janus kinases (JAKs; Yoshimura et al., 2007). This is accomplished by facilitating their degradation through an E3 ligase-like mechanism involving the recruitment of Elongin B and C with Cullin5 to catalyze the polyubiquitination of bound target proteins (Zhang et al., 1999; Kamizono et al., 2001; Babon et al., 2006). Cish has been shown to interact with the IL-2, erythropoietin, and growth hormone receptors (Landsman and Waxman, 2005) and is thought to inhibit signal transducer and activator of transcription 5 (STAT5) phosphorylation by competing with activated receptor binding sites. Nevertheless, the notion that Cish directly inhibits STAT5 phosphorylation and subsequent activation does not appear to be fully supported by the available evidence. STAT signaling is acute, with activation occurring a few minutes after receptor-ligand binding; however, many of these studies evaluated Cish-mediated suppression several hours after activation and with discordant results (Matsumoto et al., 1997; Cohney et al., 1999; Endo et al., 2003; Uyttendaele et al., 2007). Despite these provocative and thorough studies, the immunological and molecular role of Cish remains obscure and controversial.

We sought to explore the role of Cish in CD8<sup>+</sup> T cell biology and its molecular mode of action. In addition to TCR stimulation, we found that Cish expression is induced in tumor-specific T cells that have infiltrated into antigen-relevant tumors. The deletion of Cish resulted in enhanced CD8<sup>+</sup> T cell expansion, function avidity, and polycytokine release. Furthermore, the adoptive transfer of Cish-deficient CD8<sup>+</sup> T cells resulted in profound and durable regression of a poorly immunogenic established cancer. Surprisingly, no differences in STAT5 phosphorylation or activation were observed in

the absence of Cish. Instead, we uncovered a novel interaction between Cish and a principle TCR signaling component, PLC- $\gamma$ 1. Cish physically interacted with PLC- $\gamma$ 1 and targeted it for proteasomal degradation via polyubiquitination after TCR stimulation. These data reveal that Cish plays a significant role in CD8<sup>+</sup> T cell biology by attenuating TCR signaling, functional avidity, and immunity to cancer through a novel molecular mode of action.

## RESULTS

### Cish is induced upon TCR stimulation and in the tumor microenvironment

We sought to explore the role of Cish in effector T cell immunity by evaluating its expression and the consequences of its deletion. To evaluate Cish expression, we stimulated naive-enriched CD8<sup>+</sup> T cells (CD62L<sup>+</sup>CD44<sup>-</sup>) with plate-bound  $\alpha$ CD3 and evaluated mRNA and protein levels. We found that there was a basal level of Cish in naive T cells that was rapidly induced upon TCR stimulation, with expression increasing by several orders of magnitude a few hours after activation (Fig. 1, A and B). TCR stimulation initiates T cell differentiation, from naive to memory subsets. We observed a progressive increase in *Cish* mRNA upon differentiation from naive, T<sub>CM</sub> and T<sub>EM</sub> effector states after in vivo stimulation (Fig. 1 C). We confirm and extend previous studies that Cish is induced after TCR stimulation (Li et al., 2000) to CD8<sup>+</sup> T cells.

Tumor progression occurs despite the infiltration of tumor-specific T cells (Zippelius et al., 2004). We hypothesized that T cells interact with their target antigen on the tumor, and this TCR stimulation would induce Cish. To test this, we used the pmel-1 TCR transgenic tumor model, which uses a CD8<sup>+</sup> T cell model specific against the melanoma/melanocyte differentiation antigen gp100 (Overwijk et al., 2003), and evaluated Cish expression in T cell infiltrates from relevant and irrelevant tissues. We found tumor-specific T cells in the tumor 6 d after adoptive transfer of naive congenically marked pmel-1 T cells into mice bearing the 3123 melanoma line expressing gp100 on their abdomen (Acquavella et al., 2015; Fig. 1 D). The T cells in the antigen-relevant tumor, but not in the nondraining axillary lymph node, had pronounced up-regulation of Cish (Fig. 1, E and F). These findings indicate that Cish is dynamically up-regulated after TCR stimulation, progressive T cell differentiation, and in antigen-specific TILs.

To further explore the functional consequence of Cish expression in effector CD8<sup>+</sup> T cells, we generated *Cish* knockout mice and a rapid PCR-based method for genotyping the mice (Fig. 1, G and H). Surprisingly, whole-mouse immunological characterization revealed no overt changes in CD4<sup>+</sup>/CD8<sup>+</sup> cell ratios in the thymus (Fig. 1, I and J) or spleen (Fig. 1 K) between *Cish*<sup>-/-</sup> mice and age-matched WT littermates. Seeing as these mice are maintained in a pathogen-free environment, and effectively unchallenged, we hypothesized that TCR stimulation may help to delineate the role of Cish in CD8<sup>+</sup> T cells.

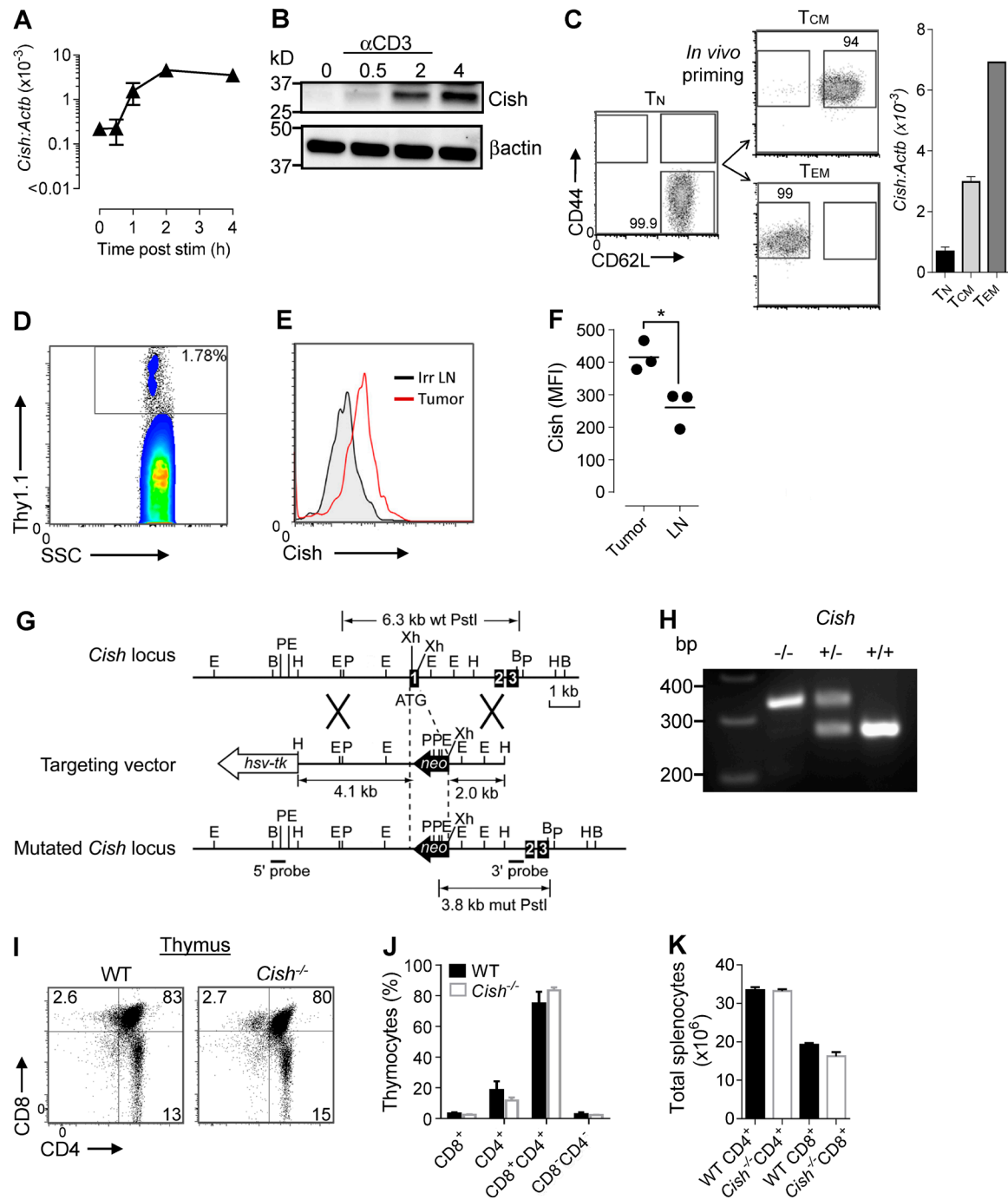


**Figure 1. Cish induction is TCR stimulation dependent.** (A) Induction of Cish gene expression using real-time PCR at indicated times after  $\alpha$ CD3 stimulation of naive CD8 $^{+}$  T cells. Results shown as means  $\pm$  SEM  $n = 3$ ; two independent experiments. (B) Western Blot of Cish protein expression after  $\alpha$ CD3 stimulation of naive CD8 $^{+}$  T cells at indicated times; three independent experiments. (C) Relative Cish mRNA expression in different CD8 $^{+}$  T cell subsets using real-time PCR; Naive (T<sub>n</sub>; CD62L $^{+}$ CD44 $^{-}$ ), in vivo-derived central memory (T<sub>cm</sub>; CD62L $^{+}$ CD44 $^{+}$ ), and effector memory (T<sub>em</sub>; CD62L $^{-}$ CD44 $^{+}$ ) after vaccination.  $n = 3$ ; three independent experiments. (D) Representative FACS blot of tumor-resident pmel-1 thy1.1 $^{+}$  CD8 $^{+}$  T cells 7 d after ACT.  $n = 3$ ; two independent experiments. (E and F) Representative FACS blot of Cish expression by intracellular staining of tissue-resident pmel-1 CD8 $^{+}$  T cells in antigen-negative non-draining axillary lymph node (Irr LN) or antigen-positive tumor 7 d after ACT. \*, P < 0.05 by unpaired Student's t test.  $n = 3$ ; two independent experiments. (G) Schematic of Cish knockout targeting construct (B, BamHI; E, EcoRI; H, HindIII; P, PstI; X, XbaI). (H) PCR confirmation of genotype. Gel electrophoresis of DNA products after PCR amplification.  $n = 300+$ . (I) Representative FACS blot of CD8 $^{+}$  and CD4 $^{+}$  thymocytes from Cish $^{-/-}$  or WT mice, enumerated in J. Values represent mean  $\pm$  SEM. P > 0.05 by unpaired Student's t test.  $n = 3$ ; three independent experiments. (K) Enumeration and flow cytometric evaluation of CD4 $^{+}$  and CD8 $^{+}$  splenocytes for each genotype. Values represent mean  $\pm$  SEM. P > 0.05 by unpaired Student's t test.  $n = 3$ ; three independent experiments.

### Cish inhibits CD8<sup>+</sup> T cell expansion, functional avidity, and cytokine polyfunctionality

To explore the role of stimulation and Cish in CD8<sup>+</sup> T cells, we isolated CD8<sup>+</sup> T cells from WT or *Cish*<sup>-/-</sup> pmel-1 mice, stimulated them with peptide-pulsed splenocytes from C57BL/6 mice, and examined proliferation and cytokine production in vitro. Flow cytometric analysis after CD8<sup>+</sup> T cell isolation revealed that the CD8<sup>+</sup> T cell differentiation state remained unaltered in the steady state with or without Cish (Fig. 2 A). Enumeration of CD8<sup>+</sup> T cells 1 wk after in vitro priming revealed significantly more T cells in the absence of Cish (Fig. 2 B). To evaluate if apoptosis accounted for this increased in vitro T cell expansion, primed T cells were TCR stimulated and stained with the nuclear stains 7-AAD and Annexin V, which bind to phosphatidylserine on the cell surface of preapoptotic cells. There was an ~50% increase in Annexin V staining on WT T cells 4 h after TCR restimulation compared with knockout T cells (Fig. 2 C). These data may help explain why there was an increase in Cish-deficient T cell expansion after TCR stimulation.

Next, we sought to determine the functional consequences of *Cish* deletion. After an overnight co-culture with primed pmel-1 T cells and titrated peptide-pulsed splenocytes, we measured cytokine levels in the supernatant using ELISA. In the absence of Cish, there was a significant increase in IFN- $\gamma$ , TNF and IL-2 levels in the supernatant as compared with co-cultured WT T cells (Fig. 2, D–F). In addition to a 100-fold increase in antigen sensitivity, we also observed a significant increase in the maximal amount of cytokine release as measured by IFN- $\gamma$ , TNF, and IL-2 levels.

ELISA's measure total cytokine levels in the supernatant and do not directly measure cytokine production on a subpopulation or cellular level. To evaluate if different subpopulations or individual T cells were responsible for this skewed increase in cytokine production, CD8<sup>+</sup> T cells were stimulated and co-stained for intracellular IFN- $\gamma$ , TNF, and IL-2. We observed an increase in both two and three cytokine-producing cells in the absence of Cish (Fig. 2, G and H). From these data, Cish appears to negatively regulate T cell cytokine production, inhibiting both effector cytokines like IFN- $\gamma$  and TNF along with supportive cytokines, such as IL-2, after TCR stimulation in vitro.

### Cish deletion or knockdown enhances CD8<sup>+</sup> T cell antitumor immunity

We sought to evaluate the in vivo functional significance of the increased in vitro expansion and functional avidity of Cish-deficient CD8<sup>+</sup> T cells. To this end, we adoptively transferred (ACT) melanoma/melanocyte-specific pmel-1 T cells with or without Cish into established B16 melanoma-bearing C57BL/6 hosts in conjunction with recombinant vaccine and IL-2, as previously described (Palmer et al., 2008). After ACT of Cish-deficient pmel-1 T cells, we observed a significant and durable regression of large, established tumors as compared with WT T cells (Fig. 3 A). This profound regression

also resulted in improved survival, with the ACT of *Cish*<sup>-/-</sup> T cells extending the survival of tumor-bearing mice by more than 60 d (Fig. 3 B). Previously, we observed a direct correlation with improved tumor clearance and increase in ocular autoimmunity when targeting the melanoma/melanocyte antigen gp100 (Palmer et al., 2008). In concordance with enhanced tumor regression, the ACT of *Cish*<sup>-/-</sup> pmel-1 T cells resulted in a significant increase in ocular autoimmunity 6 d after treatment, as compared with WT T cells (Fig. 3 C). We wanted to determine if the enhanced expansion of Cish-deficient T cells in vitro would correlate to changes in in vivo expansion. Serial sampling of treated mice after the ACT of congenically marked pmel-1 T cells revealed a pronounced expansion and delayed contraction of Cish-deficient T cells over T cells obtained from their WT littermates (Fig. 3 D). Similar to our in vitro findings, we found a significant decrease in the apoptosis of *Cish*<sup>-/-</sup> CD8<sup>+</sup> T cells in the spleen 6 d after ACT (Fig. 3 E), which may account for the increase in in vivo T cell numbers during the peak of response. Interestingly, Cish does not appear to regulate the contraction phase of an in vivo stimulation, perhaps because of a lack of antigenic stimulation and subsequent hyperactivation.

It should be noted that these tumor experiments were performed in nonirradiated, immune-replete host mice. Previously, we found that Cish deletion in CD8<sup>+</sup> T cells resulted in significantly enhanced polycytokine release (Fig. 2, E and F). There remains the possibility that increased cytokine production, in particular IL-2, may influence other adaptive immune components (Antony et al., 2005). To mitigate this potential confounder and evaluate CD8<sup>+</sup> T cell-intrinsic in vivo tumor killing, we adoptively transferred subtherapeutic numbers of pmel-1 T cells with or without Cish ( $2.5 \times 10^5$ ) into empty *Rag*<sup>1-/-</sup> B16 tumor-bearing hosts, with reduced administration of vaccine ( $10^7$  PFU) and exogenous IL-2 ( $2 \times 10^4$  IU), and then evaluated tumor growth. Remarkably, we observed the long-term maintenance with the subtherapeutic numbers of tumor-specific Cish-deficient but not the WT CD8<sup>+</sup> T cells (Fig. 4 A), with no progression of palpable tumor masses for >50 d. Interestingly, starting at ~55 d after ACT, we observed the outgrowth of clear amelanotic tumors in five of the five mice treated in two independent experiments. Presumably, the growth of this ultimately lethal depigmented mass is a result of gp100 antigen loss, perhaps through long-term tumor-pruning by Cish-deficient tumor-specific T cells (Fig. 4 B). We sought to determine if *Cish*<sup>-/-</sup> tumor-specific T cells maintained their increased functional avidity in vivo. To this end, indelibly marked pmel-1 T cells were ex vivo enriched from splenocytes with magnetic beads 7 d after transfer and evaluated for IFN- $\gamma$  release against peptide-pulsed targets (Fig. 4 C). We found an ~1000-fold increase in functional avidity of ex vivo-stimulated *Cish*<sup>-/-</sup> compared with WT T cells. Here, the IFN- $\gamma$  release of Cish-deficient T cells at 1 nM ( $10^{-9}$  M) of antigen was similar to the IFN- $\gamma$  release WT T cells at 1  $\mu$ M ( $10^{-6}$  M). This apparent maintenance of enhanced functional avidity may be important when targeting

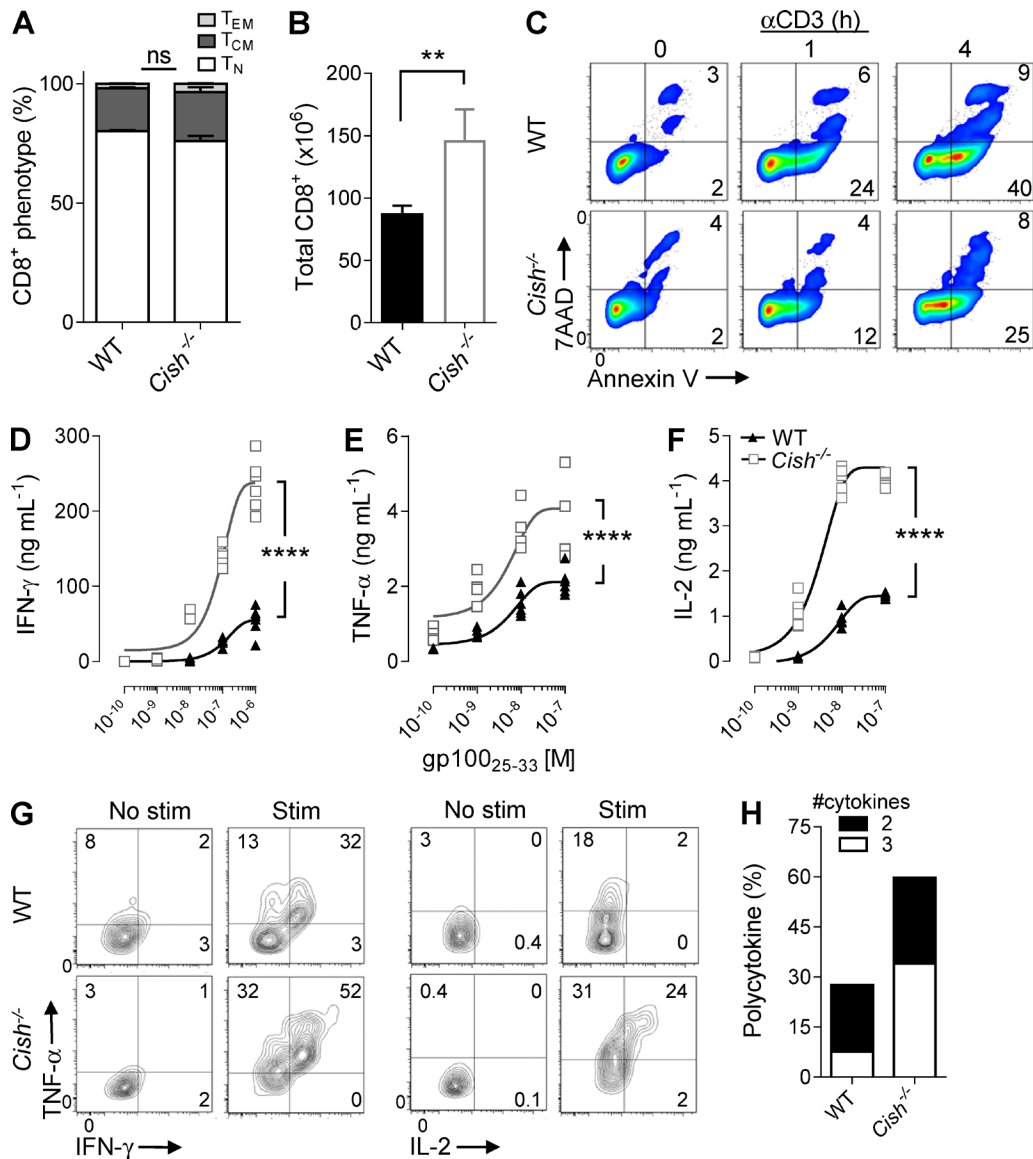


**Figure 2. Cish inhibits CD8<sup>+</sup> T cell expansion and functional avidity.** (A) Phenotypic memory analysis of CD8<sup>+</sup> T cells from Cish<sup>-/-</sup> and WT pmel-1 littermate mice using flow cytometry. Values represent mean  $\pm$  SEM. P  $> 0.05$  by unpaired Student's *t* test. *n* = 3; three independent experiments. (B) Enumeration of T cell expansion 6 d after stimulation with gp100<sub>25-33</sub> peptide-pulsed splenocytes. Values represent mean  $\pm$  SEM. \*\*, P  $< 0.01$  by unpaired Student's *t* test. *n* = 3; three independent experiments. (C) Evaluation of apoptosis of primed Cish<sup>-/-</sup> or WT CD8<sup>+</sup> T cells as assessed by flow cytometric evaluation of 7-AAD and Annexin V staining after αCD3 restimulation at times indicated. *n* = 3; three independent experiments. (D-F) Enzyme-linked immunosorbent assay (ELISA) evaluation of IFN- $\gamma$ , TNF or IL-2 in supernatants after an overnight co-culture of primed Cish<sup>-/-</sup> or WT pmel-1 CD8<sup>+</sup> T cells with peptide-pulsed splenocytes. Values are shown as means  $\pm$  SEM. \*\*\*\*, P  $< 0.0001$  by two-way ANOVA. *n* = 3; three independent experiments. (G) Representative FACS blot of intracellular IFN- $\gamma$ , TNF, and IL-2 in Cish<sup>-/-</sup> or WT pmel-1 CD8<sup>+</sup> T cells 6 h after αCD3 stimulation. *n* = 3; three independent experiments. (H) Assessment of cytokine polyfunctionality in Cish<sup>-/-</sup> or WT pmel-1 CD8<sup>+</sup> T cells from (G) using Boolean gating strategy. Data are shown as total percentage of two or three concomitant cytokines present after antigenic stimulation. *n* = 3; three independent experiments.

tumors that typically express low levels of antigen. Indeed, when we eliminated Cish<sup>-/-</sup> tumor-specific T cells even 38 d after ACT by CD8 depletion, we found a significant increase in tumor growth (Fig. 4 D). This is in stark contrast with our previous observation that WT pmel-1 T cells lose in vivo efficacy as early as 5 d after transfer (Palmer et al., 2008). From our

findings, it appears that genetic whole-body deletion of Cish significantly enhances functional avidity and licenses CD8<sup>+</sup> T cells into long-lasting tumor killers which may have important implications in memory responses to a relapsing tumor.

Our work was performed using T cells derived from germline knockouts. Yang et al. (2013) observed the development

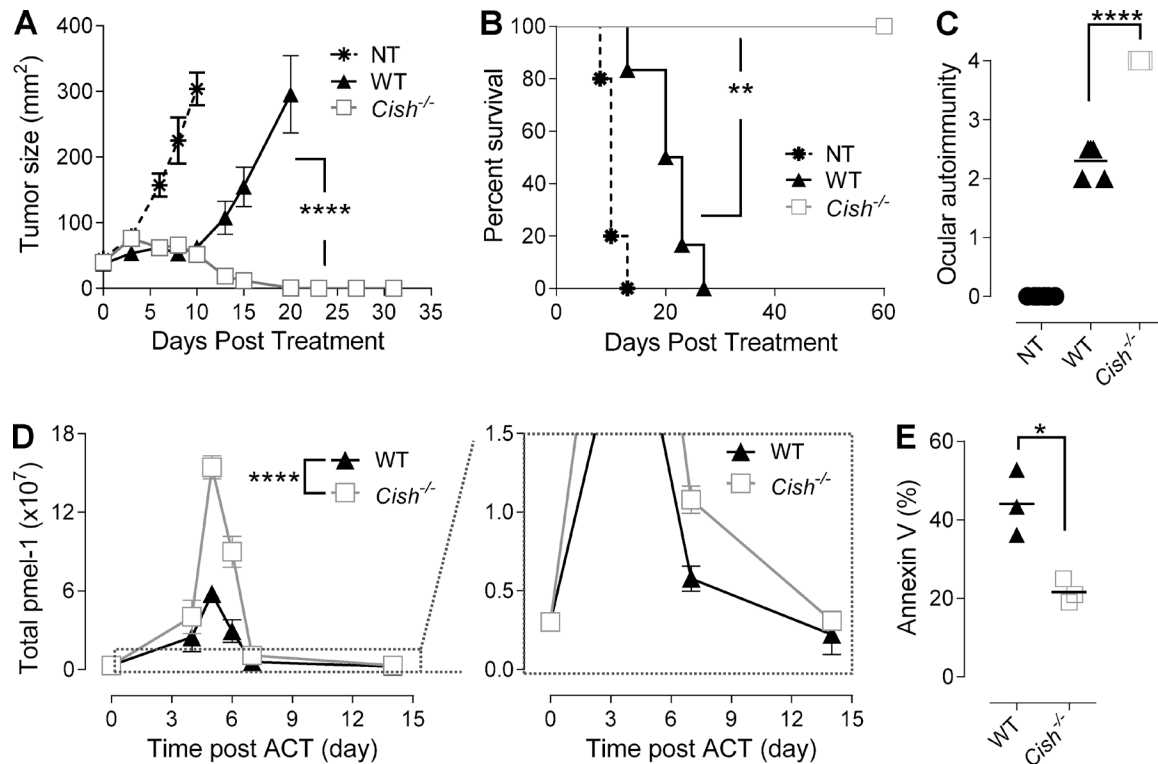


**Figure 3. Cish deletion augments CD8<sup>+</sup> T cell-mediated tumor immunity.** (A–E) 7 d after s.c. implantation of  $5 \times 10^5$  B16 melanoma cells, C57BL/6 tumor-bearing mice received the adoptive transfer (ACT) of  $10^6$  Cish<sup>-/-</sup>, WT pmel-1 naive CD8<sup>+</sup> T cells, or no cells (NT) in conjunction with rhgp100 VV (10<sup>7</sup> pfu) and IL-2 (2  $\times 10^6$  IU BID for 3 d). Tumor progression, survival, and expansion of pmel-1 T cells were followed. (A) Tumor growth as assessed by measurement of the perpendicular diameters over time. Values are shown as means  $\pm$  SEM. \*\*\*, P < 0.0001 by two-way ANOVA. n = 5 per group; 10 independent experiments. (B) Kaplan-Meier survival curve after ACT in A. \*\*, P < 0.01 by Log-rank test for trend. n = 5–6 per group; 10 independent experiments. (C) Induction of ocular autoimmunity 6 d after ACT as assessed by combinatorial scoring of severity of iridocyclitis, vitritis, and choroiditis as described in Materials and methods. \*\*\*, P < 0.0001. n = 6; two independent experiments. (D) In vivo growth kinetics of congenically marked T cells after ACT into C57BL/6 recipients as assessed by flow cytometry in conditions identical to (A). Values are shown as means  $\pm$  SEM. \*\*\*, P < 0.0001 by two-way ANOVA. n = 3; three independent experiments. (E) Ex vivo Annexin V staining by flow cytometry of congenically marked Cish<sup>-/-</sup> or WT pmel-1 T cells from the spleen 6 d after ACT. \*, P < 0.05 by unpaired Student's t test. n = 3; two independent experiments.

of lung inflammation in aged germline *Cish* knockout mice but not in T cell lineage-specific *Cish* knockout animals. Thus, there remains the possibility that a whole-body knockout might skew T cell functionality in a non-T cell–intrinsic manner. In addition, we sought to evaluate if targeting the knockout of *Cish* in tumor-specific T cells might improve tumor immunotherapy in a clinically applicable manner. To accomplish this, we knocked down *Cish* expression in WT CD8<sup>+</sup> T cells using a retrovirus encoding a short hairpin microRNA (shmiR). In concordance with T cells derived from germline knockout mice, we observed significantly enhanced CD8<sup>+</sup> T cell immune functionality both in vitro and in vivo in WT T cells expressing the shmiR-*Cish* compared with the shmiR-scramble construct (Fig. 5, A and B). To evaluate the potential clinical benefit of *CISH* knockout in patient T cells, we co-transduced shmiR-encoding retrovirus with a retrovirus encoding various tumor-specific TCRs in patient PBL and evaluated tumor reactivity using intracellular staining for IFN- $\gamma$ . Here, we found significantly enhanced specific

IFN- $\gamma$  release in tumor-specific T cells knocked down for *CISH* over that of a shmiR scramble control (Fig. 5, C–E). This was consistent for T cells specific for the cancer/testis antigen, NY-ESO-1 (Rosati et al., 2014), and the shared/melanoma antigen MART-1 (Johnson et al., 2006). Interestingly, by knocking down *CISH*, we enhanced the functionality of both the previously reported highly avid DMF5 and the poorly avid DMF4 TCRs (Johnson et al., 2006). To evaluate if the knockout of *CISH* enhanced the cytokine polyfunctionalities of tumor-specific PBL, we stained for intracellular TNF, IL-2, and IFN- $\gamma$  after a co-culture of PBL transduced with the *CISH* targeting shmiR and DMF5-TCR from Fig. 5 D with antigen-relevant tumor. Using a Boolean gating strategy, we observed a significant increase in cytokine polyfunctionalities in CD8<sup>+</sup> PBL knockout for *CISH* over that of control shmiR (Fig. 5 F). To determine if the increase in the percentage of tumor-specific T cells with *CISH* knockout correlated to increased total cytokine production, we performed an ELISA on PBL cotransduced with the *CISH*

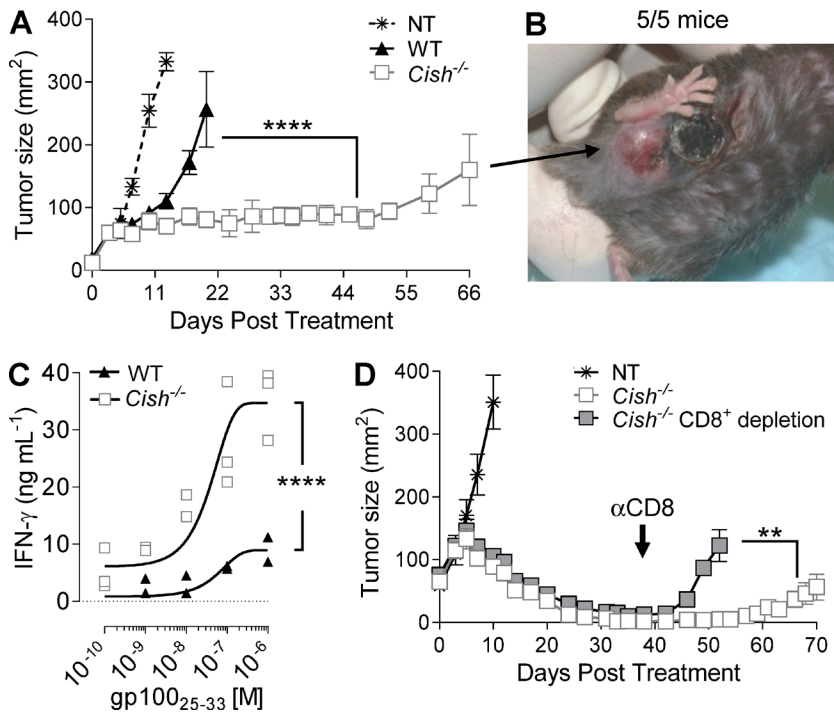


**Figure 4. Cish deletion augments long-term CD8<sup>+</sup> T cell-intrinsic tumor killing.** (A–D) Growth of B16 melanoma in *Rag1<sup>-/-</sup>* tumor-bearing hosts after ACT of  $2.5 \times 10^5$  indicated pmel-1 CD8<sup>+</sup> T cells in conjunction with rhgp100<sub>25-33</sub> (3  $\times 10^6$  pfu) and IL-2 (2  $\times 10^5$  IU BID for 3 d) or no cell transfer (NT). (A) Tumor growth as assessed by measurement of the perpendicular diameters over time. Values are shown as means  $\pm$  SEM. \*\*\*\*, P < 0.0001 by two-way ANOVA. n = 5 per group; three independent experiments. (B) Outgrowth of amelanotic tumors from A in five out of five mice, 50+ d after ACT; two independent experiments. (C) IFN- $\gamma$  production assessed by ELISA 7 d after ACT, after co-culture with ex vivo enriched congenically marked Cish<sup>-/-</sup> or WT pmel-1 T cells with cognate peptide-pulsed splenocytes. T cells were normalized for cell number. Values are shown as means  $\pm$  SEM. \*\*\*\*, P < 0.0001 by two-way ANOVA. n = 3; two independent experiments. (D) Growth of B16 melanoma in *Rag1<sup>-/-</sup>* tumor-bearing hosts as assessed by measurement of the perpendicular diameters over time after treatment. ACT of  $2.5 \times 10^5$  Cish<sup>-/-</sup> pmel-1 CD8<sup>+</sup> T cells or no cell transfer (NT) with or without administration of  $\alpha$ CD8-depleting antibody 38 d after transfer. Values are shown as means  $\pm$  SEM. \*\*, P < 0.01 by two-way ANOVA. n = 5; two independent experiments.

shmiR and MAGE-A1-specific TCR (Rao et al., 2011) with relevant and irrelevant targets. Here, we observed that the knockdown for *CISH* increased total specific IFN- $\gamma$  production in PBL specific for the cancer/testis antigen MAGE-A1 in multiple patients (Fig. 5 G). From these data, it appears that Cish negatively regulates both mouse and human T cell tumor-reactivity, though the molecular mechanism by which Cish inhibits immunity remains to be evaluated.

#### Cish inhibits global functional gene expression after TCR stimulation

Cish has been reported to compete for STAT5-binding sites on the IL-2 receptor  $\beta$  chain, inhibiting STAT5 activation (Aman et al., 1999). Surprisingly, when we evaluated STAT5 activity either after TCR stimulation (Fig. 6, A–C) or the addition of IL-2 (Fig. 6 D), we failed to observe any overt differences in STAT5 activation in the presence or absence of Cish. These efforts included STAT5 phosphorylation by Western blot, transduction of a STAT5-reporter, and IL-2 titration experiments (Fig. 6 and not depicted). Evaluation of the TCR or IL-2 receptor complex expression also yielded no discernable differences between genotypes (unpublished data). Because we did not measure any obvious changes in phosphorylation of STAT5 or levels of STAT5 activity, it was imperative for us to find an alternative explanation for the enhanced expansion, functional avidity, and tumor killing of Cish<sup>-/-</sup> T cells.

We sought to examine if the presence of Cish altered expression of prominent regulators of CD8<sup>+</sup> T cell function, proliferation, and antiapoptosis using *Tbx21*, *Cmyc*, and *Bcl2l*, respectively (Thaventhiran et al., 2013). 4 h after TCR

ligation there was a dramatic increase in all three genes in the absence of Cish, whereas up-regulation was more modest in WT T cells (Fig. 7 A). This amounted to a greater than three-fold increase in overall induction compared with WT T cells. The significant up-regulation of critical T cell effector genes in the absence of Cish led us to seek a more systematic and global evaluation of its role in acute T cell activation. Using microarray analysis, we examined relative changes in gene expression after an acute (2 h) TCR stimulation of Cish<sup>-/-</sup> and WT CD8<sup>+</sup> T cells (Fig. 7 B). We found that effector associated genes, such as *Il2*, *Prf1*, granzymes, *Myc*, *Prdm1*, and *Eomes*, were up-regulated in the absence of Cish, whereas, conversely, genes associated with naive T cells, such as *ID3*, *TCF7*, and *Bach2*, or senescent T cells, like *Cdkn1b*, (Best et al., 2013) were profoundly down-regulated in the Cish<sup>-/-</sup> T cells. The dramatic and wide-ranging changes in gene expression after stimulation prompted us to use Gene Set Enrichment Analysis (GSEA) to determine transcriptomic signatures. GSEA profiling revealed a significant association (normalized enrichment score [NES] = 8.75; P < 0.0005) between Cish deficiency and the Goldrath antigen response gene set (Goldrath et al., 2004; Fig. 7 C). We found that genes up-regulated in Cish-deficient T cells mirrored those of genes up-regulated at the peak of an antigen response of stimulated naive CD8<sup>+</sup> T cells. Conversely, we found a significant association (NES = 7.60; P < 0.0005) with genes down-regulated in naive T cells versus CD8<sup>+</sup> T cells from LCMV-challenged mice (Fig. 7 D; Kaech et al., 2002a). The dramatic and wide-ranging changes in effector gene expression after an acute TCR stimulation indicate that Cish may regulate early TCR signaling events.

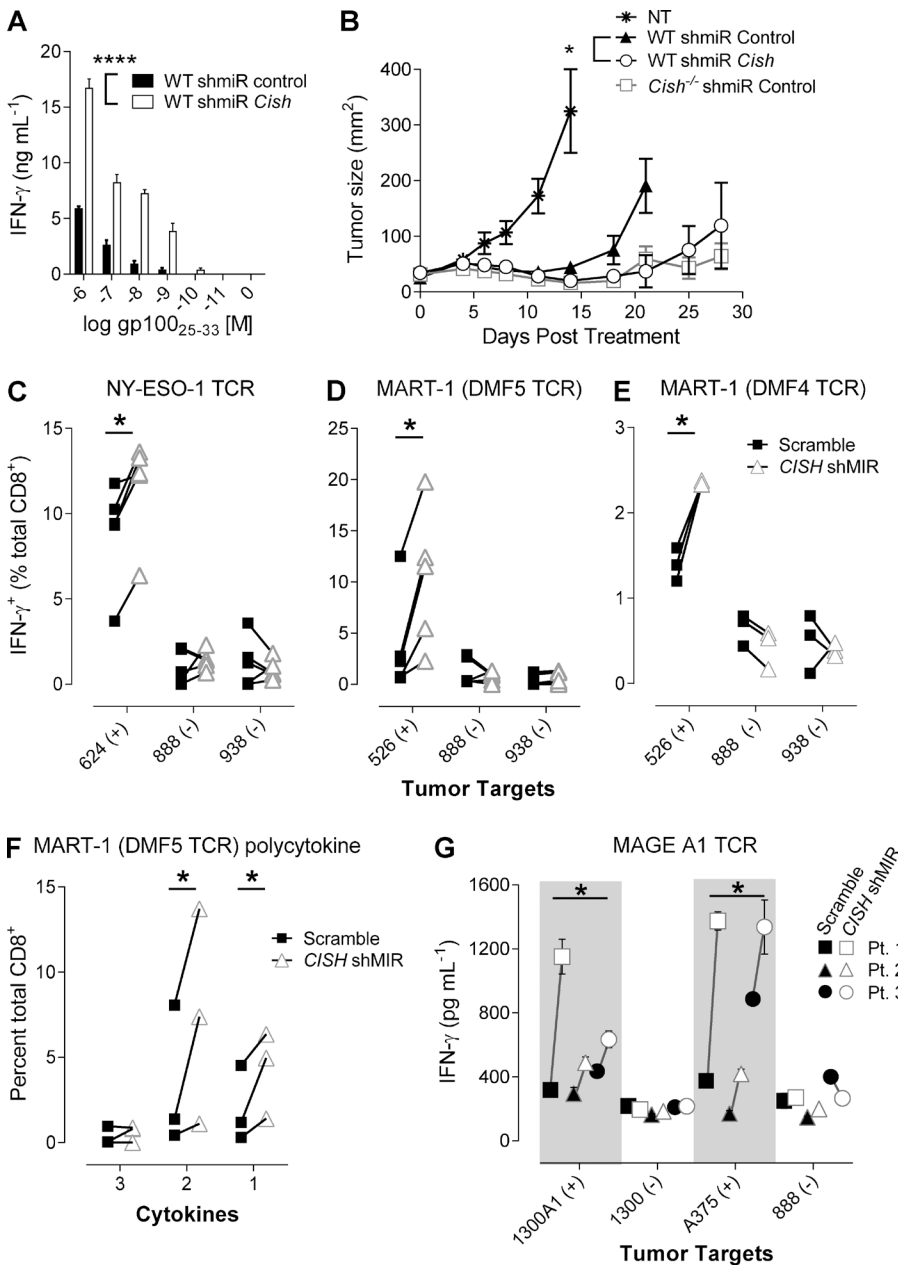


**Figure 5. Knockdown of Cish in mice and man confers enhanced CD8<sup>+</sup> T cell tumor reactivity.** (A) IFN- $\gamma$  evaluation by ELISA after an overnight co-culture of Cish shmiR or control shmiR retroviral transduced CD8<sup>+</sup> pmel-1 WT T cells. Values are shown as means  $\pm$  SEM. \*\*\*\*,  $P < 0.0001$  by two-way ANOVA.  $n = 3$ ; two independent experiments. (B) Growth of B16 melanoma in C57BL/6 tumor-bearing hosts as assessed by measurement of the perpendicular diameters over time after treatment. ACT of  $1 \times 10^6$  of retroviral transduced Cish shmiR WT, control shmiR WT, or control Cish<sup>-/-</sup> pmel-1 T cells in conjunction with rhgp100 VV ( $3 \times 10^6$  pfu) and IL-2 ( $2 \times 10^5$  IU BID for 3 d) or no cell transfer (NT). Values are shown as means  $\pm$  SEM \*,  $P < 0.05$  by two-way ANOVA.  $n = 5$ ; two independent experiments. (C–E) IFN- $\gamma$  evaluation by intracellular staining of patient PBL transduced with various tumor-specific TCRs, knocked down for CISH, and co-cultured with tumor for 6 h and assessed by flow cytometry. Retroviral transduced PBL with CISH shmiR or control shmiR and cotransduced with previously described TCR-encoding retroviruses directed against cancer-testis antigen, NY-ESO-1 (C), or MART-1 specific highly avid DMF5 (D) or poorly avid DMF4 TCR (E). 5 d after transduction, PBL were co-cultured with antigen-positive or -negative tumors and assessed for intracellular IFN- $\gamma$  by flow cytometry. \*,  $P < 0.05$  by paired Student's *t* test.  $n = 3–5$ ; three independent experiments. (F) Transduced PBL from D were co-stained for IFN- $\gamma$ , TNF, and IL-2 and evaluated for poly-cytokine functionality by flow cytometry and using a Boolean gating strategy. \*,  $P < 0.05$  by paired Student's *t* test.  $n = 3$ ; three independent experiments. (G) IFN- $\gamma$  evaluation by ELISA of patient PBL knocked down for CISH and co-cultured overnight with relevant and irrelevant tumors. Retroviral transduced PBL with CISH shmiR or control shmiR and cotransduced with TCR-encoding retroviruses directed against cancer-testis antigens, MAGE-A1. 5 d after transduction, PBL were co-cultured with antigen-positive or -negative tumors. \*,  $P < 0.05$  by paired Student's *t* test.  $n = 3$ ; two independent experiments.

### Cish inhibits TCR signaling by targeting PLC- $\gamma$ 1 for degradation

TCR stimulation triggers a cascade of tyrosine phosphorylation on downstream signaling components (Smith-Garvin et al., 2009). To explore the involvement of Cish in TCR signaling, lysates from CD8<sup>+</sup> T cells with or without Cish were blotted for phosphotyrosine after TCR stimulation (Fig. 8 A). Overall phosphotyrosine blotting revealed nominal differences, except for modestly increased intensity of bands

at  $\sim 150$  kD in Cish<sup>-/-</sup> T cells after TCR ligation (Fig. 8 B). Proteins of this apparent molecular weight correspond to the migration of PLC- $\gamma$ 1. Immunoblotting of PLC- $\gamma$ 1 and PLC- $\gamma$ 1 phosphorylated at the key Y783 activation site (Braiman et al., 2006), revealed increased intensity and duration of both variants after TCR stimulation in the absence of Cish (Fig. 8 C). Evaluation of more proximal TCR signaling components Zap-70 and LAT revealed no differences of activation in the presence or absence of Cish (Fig. 8 C).

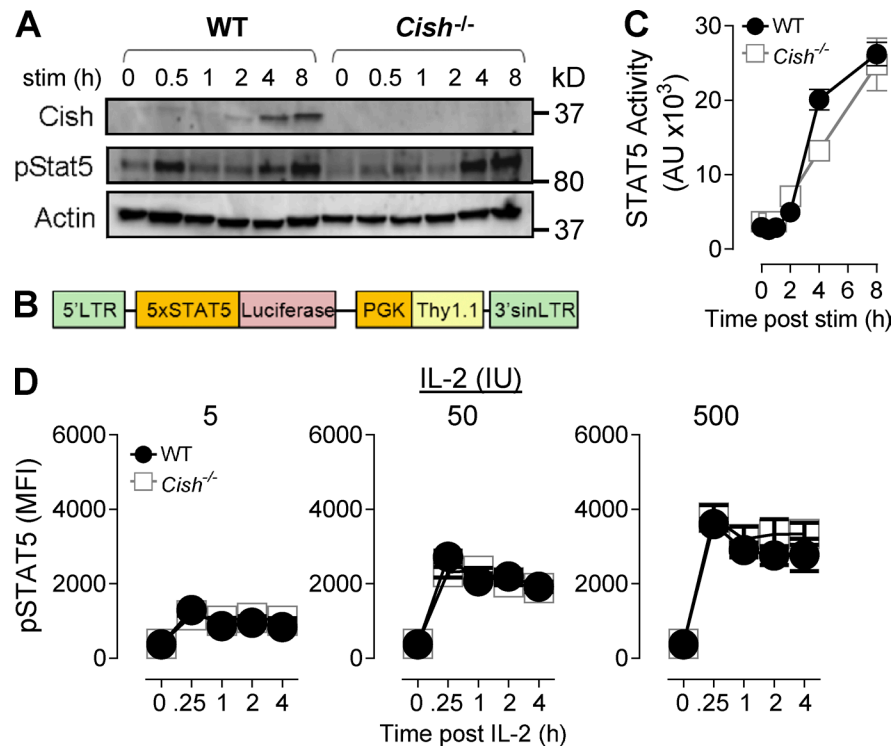


**Figure 6. No overt changes in STAT5 activation in the absence of Cish at acute time points.** (A) Western blot of Cish, phosphorylated STAT5, and  $\beta$ -actin in naive Cish<sup>-/-</sup> or WT pmel-1 T cells after  $\alpha$ CD3 stimulation at times indicated; two independent experiments. (B) Schematic of STAT5 reporter self-inactivating (sin) retrovirus coexpressing the congeneric marker Thy1.1 under the phosphoglycerate kinase 1 promoter. (C) Relative luciferase activity in STAT5 reporter-transduced Cish<sup>-/-</sup> or WT-primed pmel-1 T cells after  $\alpha$ CD3 stimulation at times indicated. Values are shown as means  $\pm$  SEM. P > 0.05 by two-way ANOVA. n = 3; two independent experiments. (D) Flow cytometric evaluation of intracellular phosphorylated STAT5 in primed Cish<sup>-/-</sup> or WT pmel-1 T cells after the addition of IL-2 at indicated concentrations and times. P > 0.05 by two-way ANOVA. n = 3; three independent experiments.

Thus, these results revealed the unexpected role of a potential Cish substrate, PLC- $\gamma$ 1, a critical cellular enzyme activated after TCR stimulation.

Activated PLC- $\gamma$ 1 converts phosphatidylinositol 4,5-bisphosphate into inositol 1,4,5-trisphosphate and diacylglycerol. These factors subsequently potentiate calcium flux and activation of PKC and other enzymes, ultimately affecting transcriptional activation of critical modulators of T cell activation: NFAT and NF- $\kappa$ B. In addition to enhanced activation of PLC- $\gamma$ 1, we also observed an increase in the magnitude and duration of  $\text{Ca}^{2+}$  release after TCR stimulation in the absence of Cish (Fig. 8 D). Furthermore, the transduction of NFAT and NF- $\kappa$ B luciferase retroviral reporters into primed CD8 $^{+}$  T cells revealed a hyperactivation of these transcription factors in Cish-deficient T cells (Fig. 8, E and F). From these data, it appears that Cish alters the signaling complex at the level of PLC- $\gamma$ 1, although its direct role is unknown.

To further determine the direct consequence of Cish on TCR signaling, we examined  $\text{Ca}^{2+}$  flux, cytokine expression, and PLC- $\gamma$ 1 activation in Cish<sup>-/-</sup> T cells reconstituted with a retrovirus expressing N-terminal FLAG-Cish or Empty cassette (Fig. 9 A). We found that Cish-reconstitution in Cish<sup>-/-</sup> T cells resulted in decreased  $\text{Ca}^{2+}$  flux (Fig. 9 B), functional

avidity (Fig. 9 C), and cytokine polyfunctionality (Fig. 9 D), emulating that of WT T cells. Cish is induced in primed T cells and there appears to be less  $\text{Ca}^{2+}$  flux in primed Cish-replete WT T cells compared with that of naive WT T cells. Not surprisingly, in the absence of Cish, there is little difference in  $\text{Ca}^{2+}$  flux between naive and primed-transduced T cells. These data are consistent with the notion that the relative expression of Cish dictates the ability of T cells to respond to antigenic stimulation. TCR-mediated signaling normally occurs in microclusters at the site of the T cell interaction with antigen-presenting cells and is detectable by confocal microscopy (Bunnell et al., 2002; Yokosuka et al., 2005). The presence of Cish specifically diminished the intensity of PLC- $\gamma$ 1 in microclusters after TCR stimulation (Fig. 9, E and F), but did not inhibit overall phosphotyrosine microcluster intensity. Cish specifically decreased the recruitment of PLC- $\gamma$ 1 to sites of TCR activation, thereby decreasing downstream TCR signaling and functional avidity.

To interrogate if Cish was physically interacting with PLC- $\gamma$ 1, YFP-tagged PLC- $\gamma$ 1 from transfected 293T cells was immunoprecipitated and then immunoblotted for Cish (Fig. 10 A). We found that Cish co-precipitated with PLC- $\gamma$ 1 and in the absence of an endogenous TCR signaling complex

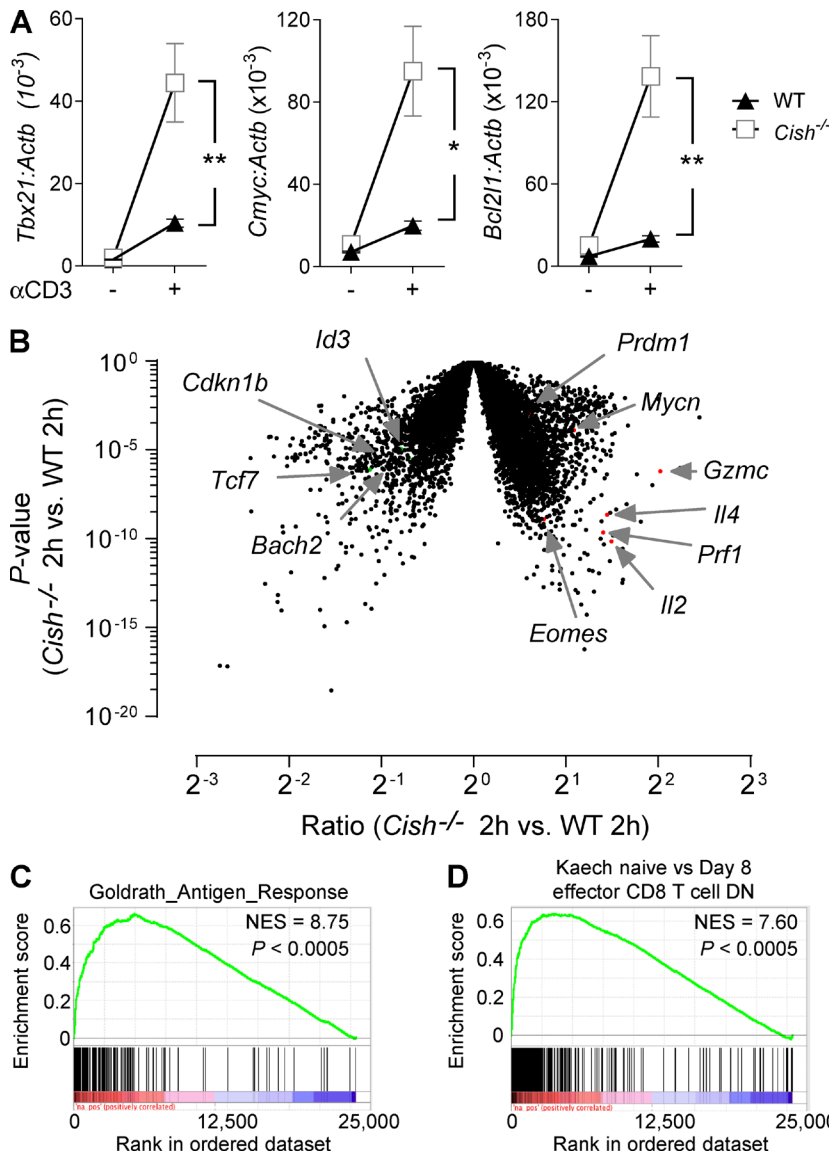


**Figure 7. TCR-dependent hyperactivation program in the absence of Cish.** (A) Enhanced up-regulation of relative *Tbx21*, *Cmyc*, and *Bcl2l1* gene expression by real-time PCR with or without  $\alpha$ CD3 stimulation for 4 h. Values are shown as means  $\pm$  SEM;  $n = 3$ . \*,  $P < 0.05$ ; \*\*,  $P < 0.01$  by two-way ANOVA.  $n = 3$ ; two independent experiments. (B) Microarray volcano plot comparing in vitro-primed *Cish*<sup>-/-</sup> or WT CD8<sup>+</sup> T cells 2 h after  $\alpha$ CD3-stimulation.  $n = 3$  independent mice per genotype; two independent experiments. (C and D) Gene-set enrichment analysis of genes in *Cish*-deficient T cells relative to WT littermates reveals a strong ranking with the Goldrath antigen response (C) and Kaech naive versus day 8 effector T cell down-regulated (D) profile.

(Fig. 10 A). To further evaluate this interaction in T cells and the role of TCR stimulation, FLAG-tagged Cish from retrovirally reconstituted *Cish*<sup>-/-</sup> CD8<sup>+</sup> T cells was immunoprecipitated and immunoblotted for PLC- $\gamma$ 1. We found that immunoprecipitation of resulted in PLC- $\gamma$ 1 co-precipitation in CD8<sup>+</sup> T cells in a stimulation-independent manner (Fig. 10 B). Importantly, we found that immunoprecipitation of endogenous Cish in unmanipulated Cish-replete WT T cells resulted in specific coimmunoprecipitation of PLC- $\gamma$ 1 (Fig. 10 C). Members of the SOCS family target proteins for proteasomal degradation via polyubiquitination (Zhang et al., 1999; Kamizono et al., 2001; Babon et al., 2006; Palmer and Restifo, 2009). Using various combinations of transfected 293T cells in the presence of the proteasome inhibitor MG-132, we found that immunoprecipitated PLC- $\gamma$ 1 was polyubiquitinated only in the presence of Cish (Fig. 10 D). To evaluate the physiological

and stimulation-dependent role of Cish in PLC- $\gamma$ 1 polyubiquitination, endogenous PLC- $\gamma$ 1 from retrovirally reconstituted Cish CD8<sup>+</sup> T cells was co-precipitated and blotted for ubiquitin. These data revealed that polyubiquitination of PLC- $\gamma$ 1 was both a Cish- and TCR stimulation-dependent process (Fig. 10 E). Further investigation using unmanipulated WT CD8<sup>+</sup> T cells confirmed that endogenous PLC- $\gamma$ 1 was strongly ubiquitinated in the presence of native Cish with TCR stimulation, whereas in the absence of TCR stimulation there was nominal PLC- $\gamma$ 1 ubiquitination and none in the complete absence of Cish (Fig. 10 F). Overall, these data demonstrate that Cish inhibits CD8<sup>+</sup> T cell expansion, functional avidity, and tumor killing, and serves as a negative feedback inhibitor of TCR signaling. This is accomplished by targeting PLC- $\gamma$ 1 for degradation via polyubiquitination, a novel mechanism of action for the SOCS family of proteins.

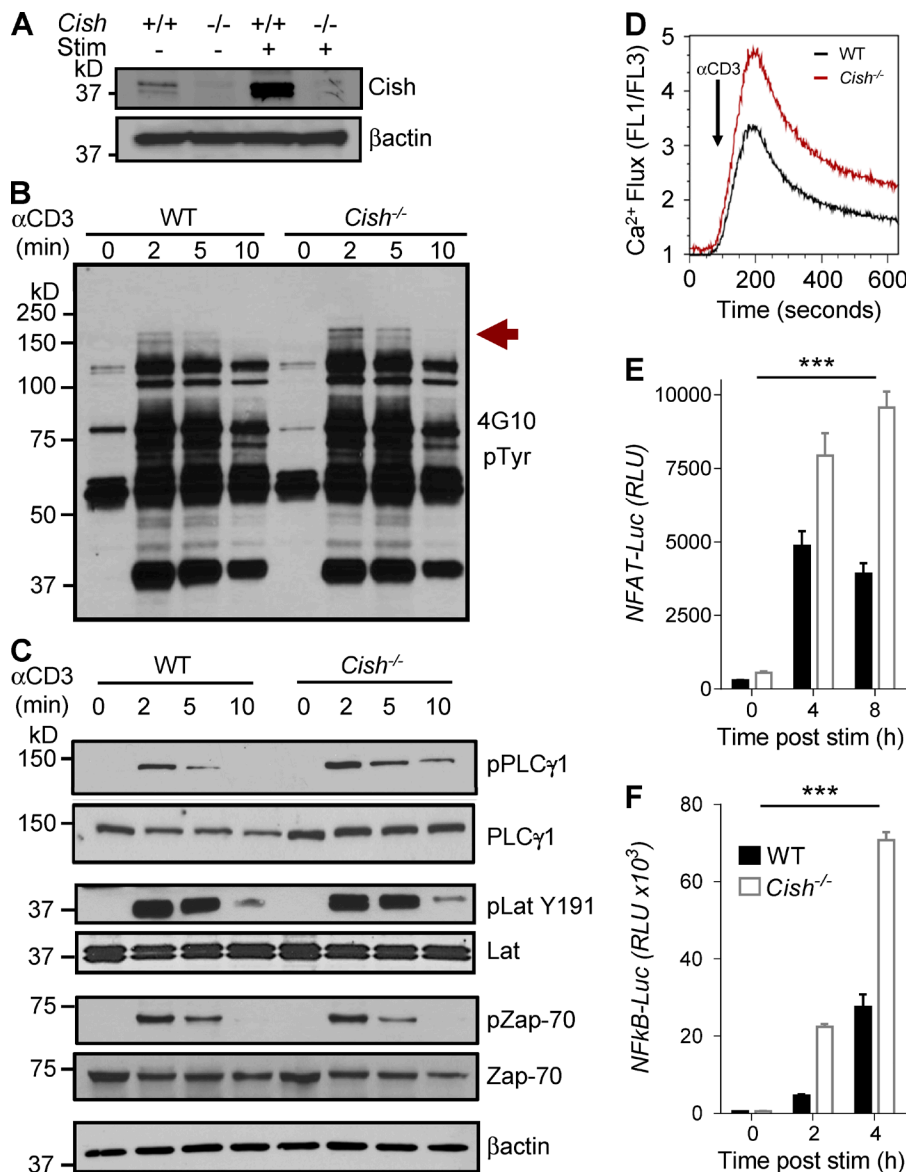


**Figure 8. Enhanced PLC- $\gamma$ 1 activation and downstream signaling in the absence of Cish.** (A) Cish protein evaluation WT or *Cish*<sup>-/-</sup> CD8<sup>+</sup> T cells with or without TCR stimulation by immunoblotting; three independent experiments. (B) Total phospho-Tyrosine (pTyr) blotting of cell lysates after  $\alpha$ CD3 stimulation of *Cish*<sup>-/-</sup> or WT CD8<sup>+</sup> T cells at times indicated by immunoblotting; three independent experiments. (C) Western blot analysis of phospho-PLC- $\gamma$ 1, total PLC- $\gamma$ 1, phospho-LAT, whole LAT, phospho-Zap-70, whole Zap-70, and  $\beta$ -actin blot after  $\alpha$ CD3 stimulation of *Cish*<sup>-/-</sup> or WT CD8<sup>+</sup> T cells at times indicated; three independent experiments. (D) Representative Ca<sup>2+</sup> flux as assessed by fluorometric evaluation after  $\alpha$ CD3 stimulation of *Cish*<sup>-/-</sup> or WT CD8<sup>+</sup> T cells. Kinetic of the ratio of Fluo3-AM by Fura Red over time shown and assessed by flow cytometry; five independent experiments. (E and F) Relative luciferase activity of NFAT and NF- $\kappa$ B reporter transduced *Cish*<sup>-/-</sup> or WT CD8<sup>+</sup> T cells after  $\alpha$ CD3 stimulation. \*\*\*, P < 0.001 by two-way ANOVA, n = 3; two independent experiments.

## DISCUSSION

Despite the abundance of T cell migration into tumors and the presence of antigen, many immunotherapies fail to elicit durable regressions. Much of the focus has been on how the tumor microenvironment suppresses the functionality of these tumor-specific T cells and approaches to overcome them (Mortarini et al., 2003; Rosenberg et al., 2005; Harlin et al., 2006; Hodi and Dranoff, 2010; Gajewski et al., 2013). Ultimately, enhancing the functional avidity of these effector T cells remains as the underlying requirement for improving therapeutic outcomes. Attempts to accomplish this have relied largely on modifying the binding capabilities of TCRs to target antigen–MHC complexes. Tactics to bypass tolerance, such as deriving TCRs from humanized HLA-transgenic mice, phage display libraries, or amino acid substitutions screens, have yielded increased TCR affinities;

however, they have uncovered additional limitations. Some of these limitations include host immunity to these de novo TCRs (Davis et al., 2010) and unforeseen off-target toxicities (Linette et al., 2013; Morgan et al., 2013). These findings highlight the need for a universally applicable means to improve the functional avidity of tumor-specific T cells. We uncovered a novel intrinsic pathway that functions to inhibit TCR signaling and downstream signaling events controlling cytokine release and T cell expansion. This negative feedback inhibition revolves around the Cish–PLC- $\gamma$ 1 axis, where Cish physically interacts with this TCR signaling intermediate and targets it for proteasomal degradation after TCR signaling. Without directly modifying TCR affinity, we were able to significantly enhance functional avidity by several orders of magnitude in the absence of spontaneous nonspecific cytokinesis. The adoptive transfer of these highly functionally avid

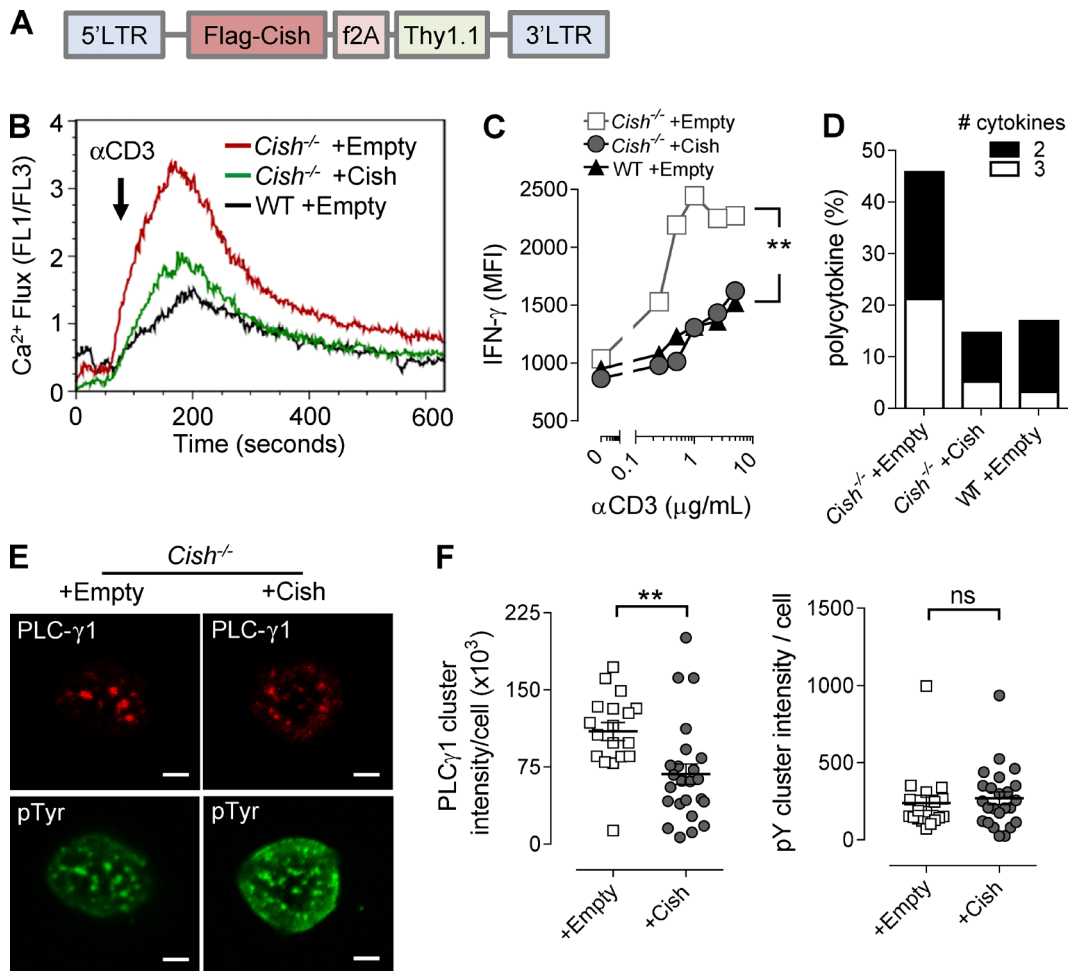


**Figure 9. Cish specifically inhibits  $\text{Ca}^{2+}$  flux, T cell polyfunctionality, and PLC- $\gamma$ 1 accumulation in TCR microclusters.** (A) Schematic of retroviral Cish expression vector. N-terminal Flag-tagged (3x) Cish, self-cleaving furin-2A (f2A) peptide, and congenic marker Thy1.1 driven by the intrinsic LTR promoter. (B) Representative  $\text{Ca}^{2+}$  flux as assessed by flow cytometry after  $\alpha\text{CD3}$  stimulation of Cish, empty control transduced Cish<sup>-/-</sup> CD8<sup>+</sup> T cells, or empty control transduced WT CD8<sup>+</sup> T cells. Kinetic of the ratio of Fluo3-AM by FuraRed over time shown and assessed by flow cytometry; four independent experiments. (C) Assessment of functional avidity by intracellular IFN- $\gamma$  using flow cytometry. Cish or empty control transduced Cish<sup>-/-</sup> CD8<sup>+</sup> T cells or empty control transduced WT CD8<sup>+</sup> T cells from B were stimulated with indicated  $\alpha\text{CD3}$  concentrations for 6 h and evaluated by flow cytometry. Values represent mean fluorescence intensity. \*\*,  $P < 0.01$  by paired Student's  $t$  test; three independent experiments. (D) Assessment of cytokine polyfunctionality in T cells from B using Boolean gating strategy. Data are shown as total percentage of two or three concomitant cytokines present after antigenic stimulation.  $n = 3$ ; three independent experiments. (E and F) Evaluation of PLC- $\gamma$ 1 and phosphotyrosine in TCR microclusters after  $\alpha\text{CD3}$  stimulation. (E) Representative confocal images from transduced CD8<sup>+</sup> T cells from B were dropped on to stimulatory coverslips, fixed after three minutes, immunostained for PLC- $\gamma$ 1 and phosphotyrosine (pTyr), and enumerated for intensity and area of each (F). Bars, 2  $\mu\text{m}$ ; ns,  $P > 0.05$ ; \*\*,  $P < 0.01$  by unpaired Student's  $t$  test.  $n = 18-24$ ; three independent experiments.

Cish-deficient or knocked down in tumor-specific CD8<sup>+</sup> T cells resulted in significant and durable regression of a poorly immunogenic, established cancer.

Great effort has been aimed at obtaining effector T cells bearing high-affinity TCRs with the notion that this will result in functionally avid T cells with enhanced in vivo tumor-killing capabilities. However, recent findings have demonstrated that de novo generated high-affinity tumor-specific T cells are deleted in effector T cell populations (Chervin et al., 2013). This work highlights the difficulty in obtaining highly avid and functionally replete T cells for adoptive immunotherapies.

In our work, we found that by targeting an intrinsic negative feedback inhibitor or TCR signaling, Cish, we were able to dramatically enhance the functional avidity and cytokine polyfunctionality of tumor-specific T cells. Furthermore, the depletion of Cish unleashed a TCR-dependent hyperactive program, resulting in the up-regulation of pro-functional, proliferative, and survival genes (*Tbx21*, *Cmyc*, and *Bcl2l1*, respectively). Interestingly, this hyperactivity was TCR dependent, in the absence of which there was no background cytokines. This is in contrast to other efforts, such as the ectopic expression of flexi-IL-12 (Kerkar et al., 2010), which resulted in high levels of basal

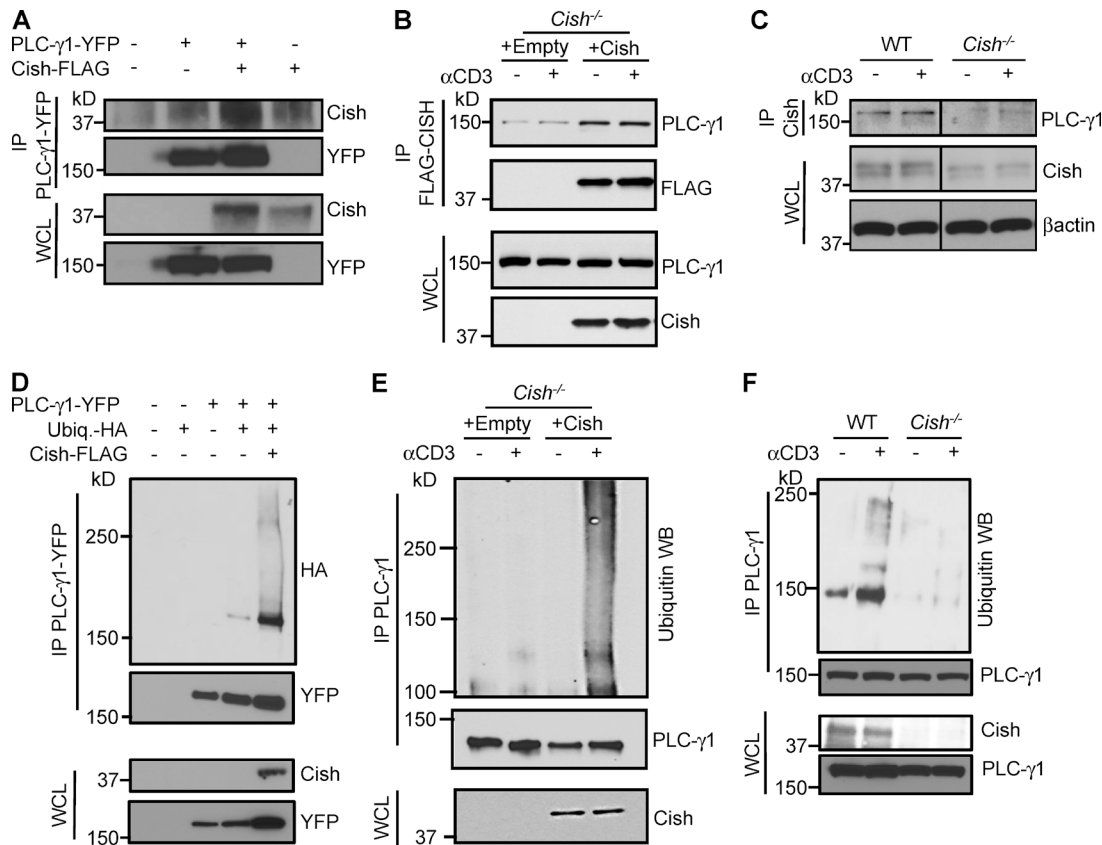


**Figure 10. TCR stimulation-dependent polyubiquitination of PLC- $\gamma$ 1 by Cish.** (A) Immunoprecipitation of YFP-tagged PLC- $\gamma$ 1 and immunoblotting of Cish in transfected 293T cells in the absence of TCR signaling complex; two independent experiments. (B) Immunoprecipitation of FLAG-tagged Cish and immunoblotting of PLC- $\gamma$ 1 in indicated transduced CD3 $^{+}$  T cells with and without CD3 stimulation (5 min). Whole lysates were blotted for PLC- $\gamma$ 1 and Cish; two independent experiments. (C) Immunoprecipitation of endogenous Cish and immunoblotting of PLC- $\gamma$ 1 in 3 d *Cish*<sup>-/-</sup> or WT CD8 $^{+}$  T cell blasts; two independent experiments. (D) 293T cells were transfected with Tagged plasmids expressing PLC- $\gamma$ 1-YFP, Ubiquitin-HA, and Cish-FLAG where indicated in the presence of the proteasome inhibitor, MG-132. After transfection, PLC- $\gamma$ 1 was immunoprecipitated and blotted for HA and YFP. Whole-cell lysates were blotted for Cish and PLC- $\gamma$ 1-YFP; two independent experiments. (E) Immunoprecipitation of endogenous PLC- $\gamma$ 1 and immunoblotting of ubiquitin in indicated reconstituted CD3 $^{+}$  T cells with or without TCR stimulation in the presence of the proteasome inhibitor, MG-132; two independent experiments. (F) Immunoprecipitation of endogenous PLC- $\gamma$ 1 and immunoblotting of ubiquitin in native CD3 $^{+}$  T cell blasts (3 d) with or without TCR stimulation in the presence of the proteasome inhibitor, MG-132; two independent experiments.

IFN- $\gamma$  release and may have nonspecific toxicities (Zhang et al., 2012). Indeed, by targeting the TCR-dependent Cish–PLC- $\gamma$ 1 signaling pathway, we observed durable tumor regression and extended survival in the absence of immune-based toxicities.

The mainstay of work with SOCS molecules has focused on how they negatively regulate their namesake, cytokine signaling (Yoshimura et al., 2007; Palmer and Restifo, 2009). Cish was first implicated as being induced by STAT5 and as potential negative regulator of STAT5 signaling (Yoshimura et al., 1995) by competing for binding sites on activated receptors (Matsumoto et al., 1997; Aman et al., 1999; Yasukawa et al., 2000; Dif et al., 2001; Endo et al., 2003; Landsman and Waxman, 2005). However, the literature regarding its immunological significance and mechanism of action has remained elusive (Cohney et al., 1999; Endo et al., 2003; Uyttendaele et al., 2007; Yoshimura, 2013). Recently, Yang et al. (2013)

showed that the deletion of Cish resulted in negative feedback inhibition of IL-4, but not IL-2. It remains unexplained how Cish might accomplish this, as no data exists regarding its ability to interact with the IL4 receptor and it contradicts previous work implicating the IL-2 receptor  $\beta$  as the site of Cish-mediated inhibition (Aman et al., 1999). The authors did demonstrate that in the absence of Cish there was increased STAT-binding occupancy to their requisite promoter elements at late time points, congruent with the observed hyperactive state and enhanced Th2 responses. Our work suggests that this significant increase in downstream effector response in *Cish*<sup>-/-</sup> T cells could be attributable to acute hyperactivation events and subsequent autocrine cytokine signaling observed at later time points. In our model, we observed that PLC- $\gamma$ 1 degradation in the presence of Cish occurred in a matter of minutes after TCR stimulation, ultimately result-

ing in decreased functional avidity and polycytokine production hours later. In retrospect, previous observations appear to support Cish as a potent novel regulator of TCR signaling and ultimately broad downstream signaling events. Our work showing that Cish targets the principle TCR-signaling intermediary PLC- $\gamma$ 1 for proteasomal-mediated degradation via polyubiquitination after TCR stimulation represents a novel pathway in SOCS-mediated negative regulation.

Although Yang et al. (2013) detected an allergic response in the whole-body *Cish*-deficient aged mice (10+ mo), T lineage-specific deletion of *Cish* had no such spontaneous phenotype. We also did not observe any overt changes in lymphopoiesis, spontaneous activation, or immunopathology in unmanipulated *Cish* knockout mice. The underlying cause of these observations might be attributable to the TCR stimulation-dependent negative regulation of PLC- $\gamma$ 1 by Cish. Cish appeared to physically interact with PLC- $\gamma$ 1 in both the steady state and after TCR stimulation, but only after TCR ligation was there a decrease in PLC- $\gamma$ 1 levels and an increase in PLC- $\gamma$ 1 polyubiquitination in the presence of Cish. These data imply that TCR ligation and subsequent downstream phosphorylation of signaling components changes the nature of the Cish-PLC- $\gamma$ 1 interaction. It's possible that the phosphorylation of PLC- $\gamma$ 1 after TCR ligation induces a conformational shift in the proximity of the Cish SH2-domain, perhaps pushing PLC- $\gamma$ 1 into the ubiquitination machinery, facilitating its degradation. The conferred specificity for PLC- $\gamma$ 1 was necessary for Cish-mediated suppression of  $\text{Ca}^{2+}$  flux and downstream cytokine release. Importantly, our experiments were done in a pathogen-free environment, and it seems plausible that the absence of Cish may result in autoimmunity in a real-world environment where infectious insults are more prevalent.

We found that the genetic deletion or the knockdown of Cish resulted in enhanced effector T cell tumor immunity. Using as few as  $2 \times 10^5$  T cells and reduced adjuvant, we observed the long-term regression and maintenance of functionality and antitumor immunity by Cish-deficient CD8 $^+$  T cells even several months after adoptive cell transfer. Indeed, only after CD8 depletion nearly a month after ACT or the late outgrowth of amelanotic tumors did mice succumb to their cancer. Although we found that Cish plays a nonredundant role in CD8 $^+$  T cell immunity, its role in CD4 $^+$  T cell immunity remains unclear. The idea that Cish depletion enables long-term tumor pruning in T cells is supported by the observation that they maintain ex vivo functionally avidity and that their depletion 30+ d after ACT resulted in tumor recrudescence. These findings are reminiscent of the work performed abrogating another TCR-negative regulator, PD1, where inhibition reversed the functionally tolerant state, enabling long-term immunity against a persistent antigen. Although it isn't clear from these data that Cish potentiates T cell exhaustion, our work does support the notion that acute signaling events dictate long-term immunity to persistent targets.

TCR signaling dictates T cell immunity to self, infection, and cancer and is consequently a highly regulated process

(Acuto et al., 2008). Increased TCR signal strength has been shown to be critical in the induction of IL-2, T-bet, Bcl-xL, and cMyc expression, leading to effector differentiation, prevention of apoptosis (Manicassamy et al., 2006; Nauerth et al., 2013), and the ability to induce tissue pathology (Dissanayake et al., 2011; King et al., 2012). We uncovered Cish as a novel negative regulator of PLC- $\gamma$ 1 and TCR signaling, unique among SOCS family molecules. PLC- $\gamma$ 1 is a key molecule in TCR signal transduction, and inhibition of its activation leads to severe impairment in T cell survival and functionality (June et al., 1990; Berg et al., 2005; Sommers et al., 2005).

After TCR ligation we observed enhanced activation of PLC- $\gamma$ 1 and downstream signaling in the absence of Cish. This enhanced downstream signaling included higher levels and duration of  $\text{Ca}^{2+}$  flux, increased NFAT and NF- $\kappa$ B transcriptional activities, a hyperactivation gene signature, and dramatic augmentation of the production of effector cytokines such as IFN- $\gamma$ , TNF and IL-2. Although it is not clear from our work that the Cish-PLC- $\gamma$ 1 axis is responsible for the enhanced *in vivo* tumor regression, the net result is increased T cell expansion, decreased apoptosis, and enhanced functional avidity in the absence of Cish. Conversely, after Cish reconstitution, there was decreased  $\text{Ca}^{2+}$  flux, functional avidity, and intensity of PLC- $\gamma$ 1 in microclusters after TCR ligation. In addition to tumor regression, enhancement of TCR signaling by depleting Cish resulted in an increase in ocular autoimmunity. This observation illustrates the need for counter-regulation of TCR signaling by Cish to restrain autoimmunity. In relation to cancer immunotherapy, it highlights the need for tumor-specific targeting without on-target toxicities (Palmer et al., 2008; Dranoff, 2013). Our findings demonstrate that proximal signaling events can have profound downstream consequences on immunity to self and cancer.

We identify Cish as an intrinsic TCR checkpoint-inhibitor with therapeutic potential. We found that the deletion or knock-down of Cish using a shRNA-encoding retrovirus significantly enhanced CD8 $^+$  T cell functionality and *in vivo* tumor killing. Cish attenuates sensitivity to TCR stimulation, inhibiting functional avidity at both low- and high-target antigen levels that may be critical for recognition of low levels of endogenously processed tumor antigens. In addition to the phenotype we observed in animal models, we found that the knockdown of CISh in patient PBL significantly enhanced their antitumor reactivity. Lastly, the activation-dependent control of PLC- $\gamma$ 1 by Cish highlights the critical nature of TCR signaling in disease processes (Gronski et al., 2004) and emphasizes the importance of temporal control of TCR signaling and T cell immunity to self and cancer (Scholer et al., 2008; Batista and Dustin, 2013; Nauerth et al., 2013). This work improves our understanding of how tumors suppress immunity, describes a novel mechanism by which a SOCS molecule interferes with TCR signaling, and unveils a new targetable interaction that may have broad immunological and therapeutic implications, particularly for ACT of low-affinity, tumor-specific T cells.

## MATERIALS AND METHODS

**Mice and cell lines and retroviral transduction.** In brief, *Cish*<sup>−/−</sup> mice were generated by targeting *Cish* in RW4 ES (129/SvJ) cells with an ~10% homologous recombination targeting efficiency. Multiple ES clones were injected, ultimately generating low and high chimeric animals and with the latter going germline. Knockouts were confirmed by performing Southern Blot analysis (PstI digest) and using the indicated probes (Fig. 1 A). Founders were then backcrossed onto C57BL/6 mice for at least eight generations. Pmel-1 Thy1.1 and pmel-1 Ly5.1 (National Cancer Institute, Frederick, MD; and The Jackson Laboratory) were crossed to *Cish*<sup>−/−</sup> mice, genotyped, and housed according to the guidelines of the Animal Care and Use Committee at the National Institutes of Health. *Cish* genotyping was performed using the following PCR primers: Cis1, 5'-GGGAGATATGGAA GATCACAG-3'; Cis2, 5'-CAGAAGGCTAGGTAACAT ATGA-3'; TKp, 5'-GCAAAACCACACTGCTCGAC-3', with expected band sizes at 326 bp for knockout and 260 bp for WT alleles. B16 melanoma was obtained from the NCI Tumor Repository and grown in 10% FCS in RPMI. Human tumor lines 526 (NY-ESO-1<sup>+</sup>, HLA-A2<sup>+</sup>), 624 (MART-1<sup>+</sup>, HLA-A2<sup>+</sup>), 888 (NY-ESO-1<sup>−</sup>, MART-1<sup>+</sup>, HLA-A2<sup>−</sup>), 928 (NY-ESO-1<sup>+</sup>, MART-1<sup>+</sup>, HLA-A2<sup>−</sup>), 1300-A1 (MAGE-A1<sup>+</sup>, HLA-A2<sup>+</sup>), 1300 (MAGE-A1<sup>−</sup>, HLA-A2<sup>+</sup>), and A375 (MAGE-A1<sup>+</sup>, HLA-A2<sup>+</sup>) were maintained in 10% FCS in DMEM. Where indicated, naive CD8<sup>+</sup> T cells were isolated from splenocytes by magnetic bead negative selection per the manufacturer's protocol (STEMCELL Technologies). Primary stimulation was accomplished using either plate-bound anti-CD3 (1 µg/ml) and soluble anti-CD28 (2 µg/ml; BD) or 0.5 µM hgp100<sub>25–33</sub> peptide-pulsed (Anaspec) splenocytes, and then cultured in RPMI with 10% FCS containing 2 ng/ml of IL-2 (Chiron Corporation) for 1 wk, as previously described (Palmer et al., 2008). Retroviral transduction was performed as described previously (Ji et al., 2011). In brief, naive CD8<sup>+</sup> enriched T cells were stimulated with plate-bound αCD3 (1 µg/ml) and soluble αCD28 (2 µg/ml) for 2 d, and then incubated on RetroNectin-coated plates with viral supernatants generated from transiently transfected PlatE cells. T cells were cultured an additional 4 d in IL-2 (60 IU), then rested overnight without IL-2 before assessment. These constructs were MSGV1-based and co-expressed the congenic marker Thy1.1 with transduction efficiencies ranging from 70 to 90%. For human transductions, similar protocols were followed, with the exception of stimulation with soluble anti-CD3 (OKT-3; 50 ng/ml), the use of 293-GP producer line and RD-114 and GALV envelopes. Efficiencies were determined using tetramer or mouse TCR constant Vβ specific antibodies and ranged from 70% to 90% efficiencies.

**Adoptive immunotherapy.** For immunotherapy, C57BL/6, Thy1.1, or *Rag1*<sup>−/−</sup> mice (Jackson Laboratories) were implanted with subcutaneous B16 melanoma (1–5 × 10<sup>5</sup> cells). At the time of ACT, 10–14 d after implantation, mice ( $n \geq$

5 for all groups unless otherwise indicated) were injected intravenously with CD8<sup>+</sup>-enriched naive or in vitro activated pmel-1 splenocytes (0.25–10<sup>6</sup> CD8<sup>+</sup> Vβ13<sup>+</sup> T cells), and 0.5–2 × 10<sup>7</sup> plaque-forming units of recombinant VV-encoding hgp100 and intraperitoneal injections of hIL-2 in PBS (6 × 10<sup>4</sup> IU/0.5 ml) twice daily for 3 d after adoptive transfer (Palmer et al., 2008). Mice were randomized, and tumors were blindly measured using digital calipers. The products of the perpendicular diameters are presented as mean ± SEM. At indicated times after ACT, spleens were harvested, ACK-lysed, enumerated, stained, and evaluated by flow cytometry as previously described (Palmer et al., 2008). Where indicated, congenically marked T cells were isolated using bead enrichment (Miltenyi Biotec or STEMCELL Technologies) from splenocytes, cell number normalized, and co-cultured cognate-peptide-pulsed syngeneic target cells from spleens.

**Flow cytometry, ELISA, microarray, and real-time PCR.** For flow cytometry, cells were stained with antibodies acquired from BD or eBioscience and processed as previously described using a FACSCanto II Flow cytometer (BD; Palmer et al., 2008). Different T cells subsets were generated after ACT of naive FACS sorted CD8<sup>+</sup> OT-1 T cells and rVV-OVA vaccination, and then isolated from splenocytes 5 d later using CD8, CD62L, CD44 staining, and high speed sorting using the FACSAria. Samples were analyzed using FlowJo software (Tree Star). For ex vivo *Cish* evaluation, naive-enriched Thy1.1<sup>+</sup> pmel-1 T cells were ACT into mice bearing 10 d 3123-hgp100 tumors on the abdomen. 6 d later tumors and irrelevant axillary lymph nodes were harvested and stained for the congenic Thy1.1<sup>+</sup> marker and intracellularly stained for *Cish*. For intracellular staining, cells were surface stained with LIVE/DEAD (Molecular Probes), then fix/permeabilized as per manufacturer's instructions (BD) and stained intracellularly for IFN-γ, TNF, and IL-2. Calcium flux was performed by co-staining T cells with Fluo3-AM and Fura Red (Molecular Probes) at 37°C for 30 min, washed three times as previously described (Chaigne-Delalande et al., 2013). For kinetics, T cells were collected for 20 s to establish baseline, then incubated with αCD3-biotin for 20 s, streptavidin cross-linking added and cells collected at times indicated. Data represented as the ratio of Fluo3/Fura-Red respective of time using FlowJo software. Cytokine quantities were determined by ELISA (R&D Systems) using supernatant from an overnight co-culture of T cells (10<sup>5</sup>) and peptide-pulsed C57BL/6 splenocytes (10<sup>5</sup>). T cells were stimulated with plate-bound anti-CD3 (1 µg/ml) for indicated times, harvested and then subjected to subsequent analysis.

For microarray, one week cultured primed T cells were stimulated with αCD3, RNA extracted and cDNA generated according to manufacturer's instructions (ABI). Gene expression levels were determined with GeneChip Mouse Gene 1.0 ST arrays according to manufacturer's protocols (Affymetrix). Real-time PCR was conducted using a two-step commercially available intron-spanning primer/probe sets (Applied Biosys-

tems) and analyzed using a CFX-96 (Bio-Rad Laboratories). Gene expression levels were calculated relative to the house-keeping gene encoding  $\beta$ -actin (*Actb*).

**Western blotting, immunoprecipitation, luminescence, and confocal microscopy.** Western blotting was performed using TGX reagents (Bio-Rad Laboratories) and protocols on nitrocellulose or PVDF paper, incubated with antibodies against FLAG, Cish, PLC- $\gamma$ 1, pPLC- $\gamma$ 1, and other listed antibodies with appropriate HRP-conjugated secondary antibodies (Cell Signaling Technology and Santa Cruz Biotechnology, Inc.). Blots were developed using chemiluminescence (Thermo Fisher Scientific), gel images were captured with the Gel Doc XRS (Bio-Rad Laboratories) and densitometry was evaluated using Quantity One software (Bio-Rad Laboratories) or by using x-ray film (Kodak). For coimmunoprecipitation, cells incubated with soluble  $\alpha$ CD3-biotin, cross-linked with streptavidin, lysed, cleared, and normalized using BCA assay (Thermo Fisher Scientific), as previously described (Guittard et al., 2015). In the ubiquitin studies, cells were cultured in the presence of proteasome inhibitor MG-132 (EMD Millipore). 293T cells were transfected with indicated plasmids using Calcium Chloride (Thermo Fisher Scientific). Cleared supernatants were applied to antibody-bound IP agarose beads and treated as per manufacturer's instructions (Santa Cruz Biotechnology, Inc.). Luminescence was performed using 20  $\mu$ l of cell culture lysis buffer, 100  $\mu$ l of luciferase reagent (Promega) as per manufacturer's instructions and evaluated using a GlowMax 96-well luminometer (Promega). Confocal images were obtained using glass slides coated with immobilized  $\alpha$ CD3 $\epsilon$  (10  $\mu$ g/ml). Samples were treated, stained and imaged as previously described (Balagopalan et al., 2011) with the following modifications: after permeabilization, cells were immunostained with primary antibodies directed to PLC- $\gamma$ 1 (Santa Cruz Biotechnology) and pTyr (4G10; EMD Millipore). The 568 channel (used for imaging anti-phosphotyrosine) was used to generate surfaces for analysis of all punctae, including number of microclusters, calculation of microcluster area, and channel intensity. The surfaces were then used to make a new channel for pixels in the 488 channel (used for imaging of PLC- $\gamma$ 1) and microcluster number, area and intensity in the newly generated channel were obtained.

**Statistics.** Averages are presented as mean  $\pm$  SEM. We performed analysis of variance (ANOVA), Student's *t* test, or Wilcoxon Rank Sum where appropriate using the StatView or GraphPad Prism software; significance considered at  $P < 0.05$ . Survival analyses and graphs were performed using GraphPad software, *p*-values were determined by Log-rank test for trend. GSEA profiling was performed using the GSEA web-based interface at the Broad Institute.

## ACKNOWLEDGMENTS

We thank A. Mixon and S. Farid of the Flow Cytometry Unit for help with flow cytometry analyses and sorting, Zhiya Yu and David Jones for technical animal

support. We would like to thank Parthav Jailwala, Eric Stahlberg, and David Goldstein from the CCRIFX core (NCI) for expert microarray analysis. The microarray data are deposited at GEO (accession number: GSE56328, <http://www.ncbi.nlm.nih.gov/geo/query/acc.cgi?acc=GSE56328>). We also wish to thank Allen Bosley, Thorkel Andresson, Jim Ihle and Evan Parganas for significant material support. Megan Luckey and Jung-Hyun Park provided excellent discussions. Supported by the Intramural Research Program of the National Cancer Institute, Center for Cancer Research of the US National Institutes of Health.

The authors declare no competing financial interests.

Author contributions: D.C. Palmer, G.C. Guittard, S.J. Patel, Z. Franco, L.E. Samelson, and N.P.R. designed research. D.C. Palmer, G.C. Guittard, R. Roychoudhuri, R. Varma, E. Wang, F.M. Marincola, and L. Balagopalan analyzed data. D.C. Palmer, G.C. Guittard, S.J. Patel, Z. Franco, Y. Ji, N. Van Panhuys, L. Gattinoni, M. Sukumar, J.G. Crompton, R.L. Eil, D. Clever, R. Roychoudhuri, A. Chichura, and R. Varma performed experiments. S.J. Patel, L.B., C.A. Klebanoff, J.G. Crompton, and R. Roychoudhuri contributed to manuscript preparation. D.C. Palmer, G.C. Guittard, L.E. Samelson, and N.P. Restifo wrote the manuscript.

Submitted: 18 February 2015

Accepted: 11 September 2015

## REFERENCES

Acquavella, N., D. Clever, Z. Yu, M. Roelke-Parker, D.C. Palmer, L. Xi, H. Flickie, Y. Ji, A. Gros, K. Hanada, et al. 2015. Type I cytokines synergize with oncogene inhibition to induce tumor growth arrest. *Cancer Immunol. Res.* 3:37–47. <http://dx.doi.org/10.1158/2326-6066.CIR-14-0122>

Acuto, O., V. Di Bartolo, and F. Michel. 2008. Tailoring T-cell receptor signals by proximal negative feedback mechanisms. *Nat. Rev. Immunol.* 8:699–712. <http://dx.doi.org/10.1038/nri2397>

Aman, M.J., T.-S. Migone, A. Sasaki, D.P. Ascherman, Mh. Zhu, E. Soldaini, K. Imada, A. Miyajima, A. Yoshimura, and W.J. Leonard. 1999. CIS associates with the interleukin-2 receptor beta chain and inhibits interleukin-2-dependent signaling. *J. Biol. Chem.* 274:30266–30272. <http://dx.doi.org/10.1074/jbc.274.42.30266>

Antony, P.A., C.A. Piccirillo, A. Akpinarli, S.E. Finkelstein, P.J. Speiss, D.R. Surman, D.C. Palmer, C.-C. Chan, C.A. Klebanoff, W.W. Overwijk, et al. 2005. CD8 $^{+}$  T cell immunity against a tumor/self-antigen is augmented by CD4 $^{+}$  T helper cells and hindered by naturally occurring T regulatory cells. *J. Immunol.* 174:2591–2601. <http://dx.doi.org/10.4049/jimmunol.174.5.2591>

Arens, R., and S.P. Schoenberger. 2010. Plasticity in programming of effector and memory CD8 T-cell formation. *Immunol. Rev.* 235:190–205.

Babon, J.J., E.J. McManus, S. Yao, D.P. DeSouza, L.A. Mielke, N.S. Sprigg, T.A. Willson, D.J. Hilton, N.A. Nicola, M. Baca, et al. 2006. The structure of SOCS3 reveals the basis of the extended SH2 domain function and identifies an unstructured insertion that regulates stability. *Mol. Cell.* 22:205–216. <http://dx.doi.org/10.1016/j.molcel.2006.03.024>

Balagopalan, L., B.A. Ashwell, K.M. Bernot, I.O. Akpan, N. Quasba, V.A. Barr, and L.E. Samelson. 2011. Enhanced T-cell signaling in cells bearing linker for activation of T-cell (LAT) molecules resistant to ubiquitylation. *Proc. Natl. Acad. Sci. USA.* 108:2885–2890. <http://dx.doi.org/10.1073/pnas.1007098108>

Batista, F.D., and M.L. Dustin. 2013. Cell:cell interactions in the immune system. *Immunol. Rev.* 251:7–12. <http://dx.doi.org/10.1111/imr.12025>

Berg, L.J., L.D. Finkelstein, J.A. Lucas, and P.L. Schwartzberg. 2005. Tec family kinases in T lymphocyte development and function. *Annu. Rev. Immunol.* 23:549–600. <http://dx.doi.org/10.1146/annurev.immunol.22.012703.104743>

Best, J.A., D.A. Blair, J. Knell, E. Yang, V. Mayya, A. Doedens, M.L. Dustin, and A.W. Goldrath. Immunological Genome Project Consortium. 2013. Transcriptional insights into the CD8 $^{+}$  T cell response to infection and

memory T cell formation. *Nat. Immunol.* 14:404–412. <http://dx.doi.org/10.1038/ni.2536>

Braiman, A., M. Barda-Saad, C.L. Sommers, and L.E. Samelson. 2006. Recruitment and activation of PLCgamma1 in T cells: a new insight into old domains. *EMBO J.* 25:774–784. <http://dx.doi.org/10.1038/sj.emboj.7600978>

Bunnell, S.C., D.I. Hong, J.R. Kardon, T. Yamazaki, C.J. McGlade, V.A. Barr, and L.E. Samelson. 2002. T cell receptor ligation induces the formation of dynamically regulated signaling assemblies. *J. Cell Biol.* 158:1263–1275. <http://dx.doi.org/10.1083/jcb.200203043>

Catlett, I.M., and S.M. Hedrick. 2005. Suppressor of cytokine signaling 1 is required for the differentiation of CD4<sup>+</sup> T cells. *Nat. Immunol.* 6:715–721. <http://dx.doi.org/10.1038/ni1211>

Chaigne-Delalande, B., F.Y. Li, G.M. O'Connor, M.J. Lukacs, P. Jiang, L. Zheng, A. Shatz, M. Biancalana, S. Pittaluga, H.F. Matthews, et al. 2013. Mg<sup>2+</sup> regulates cytotoxic functions of NK and CD8 T cells in chronic EBV infection through NKG2D. *Science.* 341:186–191. <http://dx.doi.org/10.1126/science.1240094>

Chervin, A.S., J.D. Stone, C.M. Soto, B. Engels, H. Schreiber, E.J. Roy, and D.M. Kranz. 2013. Design of T-cell receptor libraries with diverse binding properties to examine adoptive T-cell responses. *Gene Ther.* 20:634–644. <http://dx.doi.org/10.1038/gt.2012.80>

Cohney, S.J., D. Sanden, N.A. Cacalano, A. Yoshimura, A. Mui, T.S. Migone, and J.A. Johnston. 1999. SOCS-3 is tyrosine phosphorylated in response to interleukin-2 and suppresses STAT5 phosphorylation and lymphocyte proliferation. *Mol. Cell. Biol.* 19:4980–4988.

Davey, G.M., R. Starr, A.L. Cornish, J.T. Burghardt, W.S. Alexander, F.R. Carbone, C.D. Surh, and W.R. Heath. 2005. SOCS-1 regulates IL-15-driven homeostatic proliferation of antigen-naïve CD8 T cells, limiting their autoimmune potential. *J. Exp. Med.* 202:1099–1108. <http://dx.doi.org/10.1084/jem.20050003>

Davis, J.L., M.R. Theoret, Z. Zheng, C.H.J. Lamers, S.A. Rosenberg, and R.A. Morgan. 2010. Development of human anti-murine T-cell receptor antibodies in both responding and nonresponding patients enrolled in TCR gene therapy trials. *Clin. Cancer Res.* 16:5852–5861. <http://dx.doi.org/10.1158/1078-0432.CCR-10-1280>

Dif, F., E. Saunier, B. Demeneix, P.A. Kelly, and M. Edery. 2001. Cytokine-inducible SH2-containing protein suppresses PRL signaling by binding the PRL receptor. *Endocrinology.* 142:5286–5293. <http://dx.doi.org/10.1210/endo.142.12.8549>

Dissanayake, D., M.A. Gronski, A. Lin, A.R. Elford, and P.S. Ohashi. 2011. Immunological perspective of self versus tumor antigens: insights from the RIP-gp model. *Immunol. Rev.* 241:164–179. <http://dx.doi.org/10.1111/j.1600-065X.2011.01014.x>

Dranoff, G. 2013. Immunotherapy at large: Balancing tumor immunity and inflammatory pathology. *Nat. Med.* 19:1100–1101. <http://dx.doi.org/10.1038/nm.3335>

Dranoff, G., and D. Fearon. 2013. Tumour immunology. *Curr. Opin. Immunol.* 25:189–191. <http://dx.doi.org/10.1016/j.coim.2013.02.012>

Dudda, J.C., B. Salaun, Y. Ji, D.C. Palmer, G.C. Monnot, E. Merck, C. Boudousquie, D.T. Utzschneider, T.M. Escobar, R. Perret, et al. 2013. MicroRNA-155 is required for effector CD8<sup>+</sup> T cell responses to virus infection and cancer. *Immunity.* 38:742–753. <http://dx.doi.org/10.1016/j.jimmuni.2012.12.006>

Endo, T., A. Sasaki, M. Minoguchi, A. Joo, and A. Yoshimura. 2003. CIS1 interacts with the Y532 of the prolactin receptor and suppresses prolactin-dependent STAT5 activation. *J. Biochem.* 133:109–113. <http://dx.doi.org/10.1093/jb/mvg004>

Endo, T.A., M. Masuhara, M. Yokouchi, R. Suzuki, H. Sakamoto, K. Mitsui, A. Matsumoto, S. Tanimura, M. Ohtsubo, H. Misawa, et al. 1997. A new protein containing an SH2 domain that inhibits JAK kinases. *Nature.* 387:921–924. <http://dx.doi.org/10.1038/43213>

Gajewski, T.F., H. Schreiber, and Y.-X. Fu. 2013. Innate and adaptive immune cells in the tumor microenvironment. *Nat. Immunol.* 14:1014–1022. <http://dx.doi.org/10.1038/ni.2703>

Goldrath, A.W., C.J. Luckey, R. Park, C. Benoit, and D. Mathis. 2004. The molecular program induced in T cells undergoing homeostatic proliferation. *Proc. Natl. Acad. Sci. USA.* 101:16885–16890. <http://dx.doi.org/10.1073/pnas.0407417101>

Gronski, M.A., J.M. Boulter, D. Moskophidis, L.T. Nguyen, K. Holmberg, A.R. Elford, E.K. Deenick, H.O. Kim, J.M. Penninger, B. Odermatt, et al. 2004. TCR affinity and negative regulation limit autoimmunity. *Nat. Med.* 10:1234–1239. <http://dx.doi.org/10.1038/nm1114>

Guittard, G., R.L. Kortum, L. Balagopalan, N. Çuburu, P. Nguyen, C.L. Sommers, and L.E. Samelson. 2015. Absence of both Sos-1 and Sos-2 in peripheral CD4<sup>+</sup> T cells leads to PI3K pathway activation and defects in migration. *Eur. J. Immunol.* 45:2389–2395. <http://dx.doi.org/10.1002/eji.201445226>

Harlin, H., T.V. Kuna, A.C. Peterson, Y. Meng, and T.F. Gajewski. 2006. Tumor progression despite massive influx of activated CD8(+) T cells in a patient with malignant melanoma ascites. *Cancer Immunol. Immunother.* 55:1185–1197. <http://dx.doi.org/10.1007/s00262-005-0118-2>

Hilton, D.J., R.T. Richardson, W.S. Alexander, E.M. Viney, T.A. Willson, N.S. Sprigg, R. Starr, S.E. Nicholson, D. Metcalf, and N.A. Nicola. 1998. Twenty proteins containing a C-terminal SOCS box form five structural classes. *Proc. Natl. Acad. Sci. USA.* 95:114–119. <http://dx.doi.org/10.1073/pnas.95.1.114>

Hodi, F.S., and G. Dranoff. 2010. The biologic importance of tumor-infiltrating lymphocytes. *J. Cutan. Pathol.* 37:48–53. <http://dx.doi.org/10.1111/j.1600-0560.2010.01506.x>

Janicki, C.N., S.R. Jenkinson, N.A. Williams, and D.J. Morgan. 2008. Loss of CTL function among high-avidity tumor-specific CD8<sup>+</sup> T cells following tumor infiltration. *Cancer Res.* 68:2993–3000. <http://dx.doi.org/10.1158/0008-5472.CAN-07-5008>

Ji, Y., Z. Pos, M. Rao, C.A. Klebanoff, Z. Yu, M. Sukumar, R.N. Reger, D.C. Palmer, Z.A. Borman, P. Muranski, et al. 2011. Repression of the DNA-binding inhibitor Id3 by Blimp-1 limits the formation of memory CD8<sup>+</sup> T cells. *Nat. Immunol.* 12:1230–1237. <http://dx.doi.org/10.1038/ni.2153>

Jin, P., E. Wang, M. Provenzano, S. Deola, S. Selleri, J. Ren, S. Voiculescu, D. Stroncek, M.C. Panelli, and F.M. Marincola. 2006. Molecular signatures induced by interleukin-2 on peripheral blood mononuclear cells and T cell subsets. *J. Transl. Med.* 4:26. <http://dx.doi.org/10.1186/1479-5876-4-26>

Johnson, L.A., B. Heemskerk, D.J. Powell Jr., C.J. Cohen, R.A. Morgan, M.E. Dudley, P.F. Robbins, and S.A. Rosenberg. 2006. Gene transfer of tumor-reactive TCR confers both high avidity and tumor reactivity to nonreactive peripheral blood mononuclear cells and tumor-infiltrating lymphocytes. *J. Immunol.* 177:6548–6559. <http://dx.doi.org/10.4049/jimmunol.177.9.6548>

June, C.H., M.C. Fletcher, J.A. Ledbetter, G.L. Schieven, J.N. Siegel, A.F. Phillips, and L.E. Samelson. 1990. Inhibition of tyrosine phosphorylation prevents T-cell receptor-mediated signal transduction. *Proc. Natl. Acad. Sci. USA.* 87:7722–7726. <http://dx.doi.org/10.1073/pnas.87.19.7722>

Kaech, S.M., S. Hembry, E. Kersh, and R. Ahmed. 2002a. Molecular and functional profiling of memory CD8 T cell differentiation. *Cell.* 111:837–851. [http://dx.doi.org/10.1016/S0092-8674\(02\)01139-X](http://dx.doi.org/10.1016/S0092-8674(02)01139-X)

Kaech, S.M., E.J. Wherry, and R. Ahmed. 2002b. Effector and memory T-cell differentiation: implications for vaccine development. *Nat. Rev. Immunol.* 2:251–262. <http://dx.doi.org/10.1038/nri778>

Kalos, M., and C.H. June. 2013. Adoptive T cell transfer for cancer immunotherapy in the era of synthetic biology. *Immunity.* 39:49–60. <http://dx.doi.org/10.1016/j.jimmuni.2013.07.002>

Kamizono, S., T. Hanada, H. Yasukawa, S. Minoguchi, R. Kato, M. Minoguchi, K. Hattori, S. Hatakeyama, M. Yada, S. Morita, et al. 2001. The SOCS box of SOCS-1 accelerates ubiquitin-dependent proteolysis of TEL-JAK2. *J. Biol. Chem.* 276:12530–12538. <http://dx.doi.org/10.1074/jbc.M010074200>

Kerkar, S.P., P. Muranski, A. Kaiser, A. Boni, L. Sanchez-Perez, Z. Yu, D.C. Palmer, R.N. Reger, Z.A. Borman, L. Zhang, et al. 2010. Tumor-specific CD8<sup>+</sup> T cells expressing interleukin-12 eradicate established cancers in lymphodepleted hosts. *Cancer Res.* 70:6725–6734. <http://dx.doi.org/10.1158/0008-5472.CAN-10-0735>

Khor, C.C., F.O. Vannberg, S.J. Chapman, H. Guo, S.H. Wong, A.J. Walley, D. Vukcevic, A. Rautanen, T.C. Mills, K.C. Chang, et al. 2010. CIS and susceptibility to infectious diseases. *N. Engl. J. Med.* 362:2092–2101. <http://dx.doi.org/10.1056/NEJMoa0905606>

King, C.G., S. Koehli, B. Hausmann, M. Schmaler, D. Zehn, and E. Palmer. 2012. T cell affinity regulates asymmetric division, effector cell differentiation, and tissue pathology. *Immunity*. 37:709–720. <http://dx.doi.org/10.1016/j.immuni.2012.06.021>

Landsman, T., and D.J. Waxman. 2005. Role of the cytokine-induced SH2 domain-containing protein CIS in growth hormone receptor internalization. *J. Biol. Chem.* 280:37471–37480. <http://dx.doi.org/10.1074/jbc.M504125200>

Li, S., S. Chen, X. Xu, A. Sundstedt, K.M. Paulsson, P. Anderson, S. Karlsson, H.O. Sjögren, and P. Wang. 2000. Cytokine-induced Src homology 2 protein (CIS) promotes T cell receptor-mediated proliferation and prolongs survival of activated T cells. *J. Exp. Med.* 191:985–994. <http://dx.doi.org/10.1084/jem.191.6.985>

Linette, G.P., E.A. Stadtmauer, M.V. Maus, A.P. Rapoport, B.L. Levine, L. Emery, L. Litzky, A. Bagg, B.M. Carreno, P.J. Cimino, et al. 2013. Cardiovascular toxicity and titin cross-reactivity of affinity-enhanced T cells in myeloma and melanoma. *Blood*. 122:863–871. <http://dx.doi.org/10.1182/blood-2013-03-490565>

Malecek, K., S. Zhong, K. McGary, C. Yu, K. Huang, L.A. Johnson, S.A. Rosenberg, and M. Krogsgaard. 2013. Engineering improved T cell receptors using an alanine-scan guided T cell display selection system. *J. Immunol. Methods*. 392:1–11. <http://dx.doi.org/10.1016/j.jim.2013.02.018>

Manicassamy, S., S. Gupta, Z. Huang, and Z. Sun. 2006. Protein kinase C-theta-mediated signals enhance CD4<sup>+</sup> T cell survival by up-regulating Bcl-xL. *J. Immunol.* 176:6709–6716. <http://dx.doi.org/10.4049/jimmunol.176.11.6709>

Matsumoto, A., M. Masuhara, K. Mitsui, M. Yokouchi, M. Ohtsubo, H. Misawa, A. Miyajima, and A. Yoshimura. 1997. CIS, a cytokine inducible SH2 protein, is a target of the JAK-STAT5 pathway and modulates STAT5 activation. *Blood*. 89:3148–3154.

Maus, M.V., J.A. Fraietta, B.L. Levine, M. Kalos, Y. Zhao, and C.H. June. 2014. Adoptive immunotherapy for cancer or viruses. *Annu. Rev. Immunol.* 32:189–225. <http://dx.doi.org/10.1146/annurev-immunol-032713-120136>

Morgan, R.A., N. Chinnasamy, D. Abate-Daga, A. Gros, P.F. Robbins, Z. Zheng, M.E. Dudley, S.A. Feldman, J.C. Yang, R.M. Sherry, et al. 2013. Cancer regression and neurological toxicity following anti-MAGE-A3 TCR gene therapy. *J. Immunother.* 36:133–151. <http://dx.doi.org/10.1097/CJI.0b013e3182829903>

Mortarini, R., A. Piris, A. Maurichi, A. Molla, I. Bersani, A. Bono, C. Bartoli, M. Santinami, C. Lombardo, F. Ravagnani, et al. 2003. Lack of terminally differentiated tumor-specific CD8<sup>+</sup> T cells at tumor site in spite of anti-tumor immunity to self-antigens in human metastatic melanoma. *Cancer Res.* 63:2535–2545.

Naka, T., M. Narazaki, M. Hirata, T. Matsumoto, S. Minamoto, A. Aono, N. Nishimoto, T. Kajita, T. Taga, K. Yoshizaki, et al. 1997. Structure and function of a new STAT-induced STAT inhibitor. *Nature*. 387:924–929. <http://dx.doi.org/10.1038/43219>

Nauerth, M., B. Weißbrich, R. Knall, T. Franz, G. Dössinger, J. Bet, P.J. Paszkiewicz, L. Pfeifer, M. Bunse, W. Uckert, et al. 2013. TCR-ligand koff rate correlates with the protective capacity of antigen-specific CD8<sup>+</sup> T cells for adoptive transfer. *Sci. Transl. Med.* 5:192ra87.

Ohashi, P.S., S. Oehen, K. Buerki, H. Pircher, C.T. Ohashi, B. Odermatt, B. Malissen, R.M. Zinkernagel, and H. Hengartner. 1991. Ablation of “tolerance” and induction of diabetes by virus infection in viral antigen transgenic mice. *Cell*. 65:305–317.

Overwijk, W.W., M.R. Theoret, S.E. Finkelstein, D.R. Surman, L.A. de Jong, F.A. Vyth-Dreese, T.A. Dellemijn, P.A. Antony, P.J. Spiess, D.C. Palmer, et al. 2003. Tumor regression and autoimmunity after reversal of a functionally tolerant state of self-reactive CD8<sup>+</sup> T cells. *J. Exp. Med.* 198:569–580. <http://dx.doi.org/10.1084/jem.20030590>

Palmer, D.C., and N.P. Restifo. 2009. Suppressors of cytokine signaling (SOCS) in T cell differentiation, maturation, and function. *Trends Immunol.* 30:592–602. <http://dx.doi.org/10.1016/j.it.2009.09.009>

Palmer, D.C., C.C. Chan, L. Gattinoni, C. Wrzesinski, C.M. Paulos, C.S. Hinrichs, D.J. Powell Jr., C.A. Klebanoff, S.E. Finkelstein, R.N. Fariss, et al. 2008. Effective tumor treatment targeting a melanoma/melanocyte-associated antigen triggers severe ocular autoimmunity. *Proc. Natl. Acad. Sci. USA*. 105:8061–8066. <http://dx.doi.org/10.1073/pnas.0710929105>

Rabinovich, G.A., D. Gabrilovich, and E.M. Sotomayor. 2007. Immunosuppressive strategies that are mediated by tumor cells. *Annu. Rev. Immunol.* 25:267–296. <http://dx.doi.org/10.1146/annurev.immunol.25.022106.141609>

Rao, M., N. Chinnasamy, J.A. Hong, Y. Zhang, M. Zhang, S. Xi, F. Liu, V.E. Marquez, R.A. Morgan, and D.S. Schrump. 2011. Inhibition of histone lysine methylation enhances cancer-testis antigen expression in lung cancer cells: implications for adoptive immunotherapy of cancer. *Cancer Res.* 71:4192–4204. <http://dx.doi.org/10.1158/0008-5472.CAN-10-2442>

Restifo, N.P., M.E. Dudley, and S.A. Rosenberg. 2012. Adoptive immunotherapy for cancer: harnessing the T cell response. *Nat. Rev. Immunol.* 12:269–281. <http://dx.doi.org/10.1038/nri3191>

Rosati, S.F., M.R. Parkhurst, Y. Hong, Z. Zheng, S.A. Feldman, M. Rao, D. Abate-Daga, R.E. Beard, H. Xu, M.A. Black, et al. 2014. A novel murine T-cell receptor targeting NY-ESO-1. *J. Immunother.* 37:135–146. <http://dx.doi.org/10.1097/CJI.0000000000000019>

Rosenberg, S.A., R.M. Sherry, K.E. Morton, W.J. Scharfman, J.C. Yang, S.L. Topalian, R.E. Royal, U. Kammula, N.P. Restifo, M.S. Hughes, et al. 2005. Tumor progression can occur despite the induction of very high levels of self/tumor antigen-specific CD8<sup>+</sup> T cells in patients with melanoma. *J. Immunol.* 175:6169–6176. <http://dx.doi.org/10.4049/jimmunol.175.9.6169>

Scholer, A., S. Hugues, A. Boissonnas, L. Fettler, and S. Amigorena. 2008. Intercellular adhesion molecule-1-dependent stable interactions between T cells and dendritic cells determine CD8<sup>+</sup> T cell memory. *Immunity*. 28:258–270. <http://dx.doi.org/10.1016/j.immuni.2007.12.016>

Seki, Y., H. Inoue, N. Nagata, K. Hayashi, S. Fukuyama, K. Matsumoto, O. Komine, S. Hamano, K. Himeno, K. Inagaki-Obara, et al. 2003. SOCS-3 regulates onset and maintenance of T(H)2-mediated allergic responses. *Nat. Med.* 9:1047–1054. <http://dx.doi.org/10.1038/nm896>

Smith-Garvin, J.E., G.A. Koretzky, and M.S. Jordan. 2009. T cell activation. *Annu. Rev. Immunol.* 27:591–619. <http://dx.doi.org/10.1146/annurev.immunol.021908.132706>

Sommers, C.L., J. Lee, K.L. Steiner, J.M. Gurson, C.L. Depersis, D. El-Khoury, C.L. Fuller, E.W. Shores, P.E. Love, and L.E. Samelson. 2005. Mutation of the phospholipase C-gamma1-binding site of LAT affects both positive and negative thymocyte selection. *J. Exp. Med.* 201:1125–1134. <http://dx.doi.org/10.1084/jem.20041869>

Starr, R., T.A. Willson, E.M. Viney, L.J. Murray, J.R. Rayner, B.J. Jenkins, T.J. Gonda, W.S. Alexander, D. Metcalf, N.A. Nicola, and D.J. Hilton. 1997. Cish silences TCR to maintain tumor tolerance | Palmer et al.

A family of cytokine-inducible inhibitors of signalling. *Nature*. 387:917–921. <http://dx.doi.org/10.1038/43206>

Taleb, S., M. Romain, B. Ramkhelawon, C. Uyttenhove, G. Pasterkamp, O. Herbin, B. Esposito, N. Perez, H. Yasukawa, J. Van Snick, et al. 2009. Loss of SOCS3 expression in T cells reveals a regulatory role for interleukin-17 in atherosclerosis. *J. Exp. Med.* 206:2067–2077. <http://dx.doi.org/10.1084/jem.20090545>

Tanaka, K., K. Ichiyama, M. Hashimoto, H. Yoshida, T. Takimoto, G. Takaesu, T. Torisu, T. Hanada, H. Yasukawa, S. Fukuyama, et al. 2008. Loss of suppressor of cytokine signaling 1 in helper T cells leads to defective Th17 differentiation by enhancing antagonistic effects of IFN- $\gamma$  on STAT3 and Smads. *J. Immunol.* 180:3746–3756. <http://dx.doi.org/10.4049/jimmunol.180.6.3746>

Thaventhiran, J.E., D.T. Fearon, and L. Gattinoni. 2013. Transcriptional regulation of effector and memory CD8 $^{+}$  T cell fates. *Curr. Opin. Immunol.* 25:321–328. <http://dx.doi.org/10.1016/j.co.2013.05.010>

Tong, H.V., N.L. Toan, H. Song, P.G. Kremsner, J.F. Kun, and V. Tp. 2012. Association of CISH -292A/T genetic variant with hepatitis B virus infection. *Immunogenetics*. 64:261–265. <http://dx.doi.org/10.1007/s00251-011-0584-y>

Uyttdaele, I., I. Lemmens, A. Verhee, A.S. De Smet, J. Vandekerckhove, D. Lavens, F. Peelman, and J. Tavernier. 2007. Mammalian protein-protein interaction trap (MAPPIT) analysis of STAT5, CIS, and SOCS2 interactions with the growth hormone receptor. *Mol. Endocrinol.* 21:2821–2831. <http://dx.doi.org/10.1210/me.2006-0541>

Vazquez-Cintron, E.J., N.R. Monu, and A.B. Frey. 2010. Tumor-induced disruption of proximal TCR-mediated signal transduction in tumor-infiltrating CD8 $^{+}$  lymphocytes inactivates antitumor effector phase. *J. Immunol.* 185:7133–7140. <http://dx.doi.org/10.4049/jimmunol.1001157>

Whiteside, T.L. 2006. Immune suppression in cancer: effects on immune cells, mechanisms and future therapeutic intervention. *Semin. Cancer Biol.* 16:3–15. <http://dx.doi.org/10.1016/j.semcan.2005.07.008>

Yang, X.O., H. Zhang, B.S. Kim, X. Niu, J. Peng, Y. Chen, R. Kerketta, Y.H. Lee, S.H. Chang, D.B. Corry, et al. 2013. The signaling suppressor CIS controls proallergic T cell development and allergic airway inflammation. *Nat. Immunol.* 14:732–740. <http://dx.doi.org/10.1038/ni.2633>

Yasukawa, H., A. Sasaki, and A. Yoshimura. 2000. Negative regulation of cytokine signaling pathways. *Annu. Rev. Immunol.* 18:143–164. <http://dx.doi.org/10.1146/annurev.immunol.18.1.143>

Yokosuka, T., K. Sakata-Sogawa, W. Kobayashi, M. Hiroshima, A. Hashimoto-Tane, M. Tokunaga, M.L. Dustin, and T. Saito. 2005. Newly generated T cell receptor microclusters initiate and sustain T cell activation by recruitment of Zap70 and SLP-76. *Nat. Immunol.* 6:1253–1262. <http://dx.doi.org/10.1038/ni1272>

Yoshimura, A. 2013. CIS: the late-blooming eldest son. *Nat. Immunol.* 14:692–694. <http://dx.doi.org/10.1038/ni.2645>

Yoshimura, A., T. Ohkubo, T. Kiguchi, N.A. Jenkins, D.J. Gilbert, N.G. Copeland, T. Hara, and A. Miyajima. 1995. A novel cytokine-inducible gene CIS encodes an SH2-containing protein that binds to tyrosine-phosphorylated interleukin 3 and erythropoietin receptors. *EMBO J.* 14:2816–2826.

Yoshimura, A., T. Naka, and M. Kubo. 2007. SOCS proteins, cytokine signalling and immune regulation. *Nat. Rev. Immunol.* 7:454–465. <http://dx.doi.org/10.1038/nri2093>

Zhang, N., and M.J. Bevan. 2011. CD8 $^{+}$  T cells: foot soldiers of the immune system. *Immunity*. 35:161–168. <http://dx.doi.org/10.1016/j.immuni.2011.07.010>

Zhang, J.G., A. Farley, S.E. Nicholson, T.A. Willson, L.M. Zugaro, R.J. Simpson, R.L. Moritz, D. Cary, R. Richardson, G. Hausmann, et al. 1999. The conserved SOCS box motif in suppressors of cytokine signaling binds to elongins B and C and may couple bound proteins to proteasomal degradation. *Proc. Natl. Acad. Sci. USA*. 96:2071–2076. <http://dx.doi.org/10.1073/pnas.96.5.2071>

Zhang, L., S.A. Feldman, Z. Zheng, N. Chinnasamy, H. Xu, A.V. Nahvi, M.E. Dudley, S.A. Rosenberg, and R.A. Morgan. 2012. Evaluation of  $\gamma$ -retroviral vectors that mediate the inducible expression of IL-12 for clinical application. *J. Immunother.* 35:430–439. <http://dx.doi.org/10.1097/CJI.0b013e31825898e8>

Zhao, Y., A.D. Bennett, Z. Zheng, Q.J. Wang, P.F. Robbins, L.Y.L. Yu, Y. Li, P.E. Molloy, S.M. Dunn, B.K. Jakobsen, et al. 2007. High-affinity TCRs generated by phage display provide CD4 $^{+}$  T cells with the ability to recognize and kill tumor cell lines. *J. Immunol.* 179:5845–5854. <http://dx.doi.org/10.4049/jimmunol.179.9.5845>

Zippelius, A., P. Batard, V. Rubio-Godoy, G. Bioley, D. Liénard, F. Lejeune, D. Rimoldi, P. Guillaume, N. Meidenbauer, A. Mackensen, et al. 2004. Effector function of human tumor-specific CD8 T cells in melanoma lesions: a state of local functional tolerance. *Cancer Res.* 64:2865–2873. <http://dx.doi.org/10.1158/0008-5472.CAN-03-3066>